CRUDE PEROXIDASE EXTRACT FROM ONION: ACTIVITY ON O-DIPHENOL & PENTAHYDROXY CHALCONE OXIDATIVE CYCLISATION INTO AUREUSIDIN

BY

SONIA MOUSSOUNI

CHANIA, GREECE

2009

Acknowledgements

I would like to express my gratitude first of all to God who created me and made me what I am today. I would like to give special thansk and gratitude to my parents ***Mr Amar Moussouni*** *and* ***Mrs Hassina Moussouni*** *for all they did and will do for me all my life, to my dearest brother* ***Soufiene*** *and sisters* ***Sabrina****,* ***Lamia*** *and* ***Ahlem*** *for all their love and support they provide me with. I would like to give special thanks to my friend* ***Miss Amel Yamoune*** *for her help, friendship and support she provides me during this last two years in MAICh.*

I would like to express my grateful thanks to my supervisors ***Dr. Panagiotis Kefalas****, Scientific Coordinator of the Department of Food Quality and Chemistry of Natural Products,* ***Dr. Dimitris P. Makris*** *from the Department of Food Quality and Chemistry of Natural Products and* ***Dr. Anastasia Detsi,*** *Laboratory of Organic Chemistry, School of Chemical Engineering, National Technical University of Athens for their support and help during this work and for the excellent working conditions they provided me with.*

*I acknowledge the International Centre of Advanced Mediterranean Agronomic Studies (****CIHEAM****) and the director of the Mediterranean Agronomic Institute of Chania (****MAICh****),* ***Mr****.* ***Alkinoos Nikolaidis****, for giving me the opportunity to carry out my M.Sc. studies at the Institute.*

Abstract

The objective of this study was to investigate the enzymic activity of a crude onion peroxidase extract on o-diphenols and to optimise thereof the conditions for the oxidative cyclisation of pentahydroxy chalcone into the corresponding aurone (aureusidin); the reaction in question has already been observed in-house during previous studies.

Protocatechuic acid (PA) was first used as the *o*-phenol substrate structure. The enzyme showed optimum activity at 30°C, pH 6, H_2O_2 concentration of 0.8mM and substrate concentration of 2mM. Using response surface methodology the enzymic reaction was further fine tuned in view of optimising the reaction conditions for the preparation of aureusidin from the precursor pentahydroxy chalcone, the point here being that the chalcone is still an ortho diphenol system, but much more subtle than PA. An experimental setup based on a 2^3-full factorial, central composite design was implemented. The factors considered were pH, incubation time and temperature, and the model obtained produced a satisfactory fitting of the experimental data with regard to (R^2 = 0.95, p = 0.0083). The highest yield was theoretically predicted to be 308.65±43.802 expressed as the peak area, under optimal conditions (pH 5, 30°C and 5h). A scale up reaction that was carried out using the predicted optimal conditions led indeed to a high yield synthesis of aureusidin. However, an unexpected dimer of high regiospecificity (non-aromatic C sp^2-sp^2 coupling) was also isolated, the yield of which was time-dependent.

The conclusion is that indeed the crude onion POD enzyme extract may be used and further studied for the synthesis of fine chemicals, as a green and cheap alternative in the frame of organic synthetic chemistry.

Table of contents

List of figures

List of tables

List of abbreviations

4-AAP	4-Aminoantipyrine
CoA	Coenzyme A
DHC	Dihydroxy chalcone
FA	Ferulic acid
GYG	Glycine-Tyrosine-Glycine
HRP	Horse Radish Peroxidase
IAA	Indole-3-acetic acid
LC/DAD/MS	Liquid Chromatography Diode Array Mass Spectroscopy
PA	Protocatechuic acid
PCD	Programmed Cell Death
PHC	Pentahydroxy chalcone
POD	Peroxidase
POXs	Plant peroxidases
PPO	Polyphenol oxidase
THC	Tetrahydroxy chalcone

INTRODUCTION

Introduction

Polyphenols are considered as potent antioxidants for their contribution to the protection of cell constituents against oxidative damage and therefore, limit the risk of various degenerative diseases associated to oxidative stress such as cardiovascular disease, cancer, osteoporosis, diabetes mellitus and neurodegenerative disease (Lopez-Molina et *al.*, 2003). On the other hand, large quantities of both liquid and solid wastes are produced annually by the food processing industry. These waste materials contain principally biodegradable organic matter and their disposal creates serious environmental problems. New approaches aim at converting the waste materials into bio-fuels, food ingredients and other added-value bio-products (Kefalas and Makris, 2005). From this point of view the idea of using enzymes from the waste sources for use in chemical synthesis and bioremediation has emerged since they have several advantages over conventional physical and chemical treatment process (Osman and *al.*, 2008)

It should be underlined that the possibility of using the enzymes as crude extracts (ie without long and toilsome purifications) is an input of added value novelty. Peroxidases from HRP, tobacco and *Arrabidopsis thaliana* have been mostly investigated as reagents for organic synthesis and biotransformation as well as in coupled enzyme assays, chemiluminescent assays and immunoassays. Some indicative applications are: oxidative decarboxylation of auxin opening routes for new potential drugs for cancer therapy; N- and O-dealkylation; oxidative coupling; selective hydroxylation and oxygen-transfer reactions; formation of dityrosines and higher oligomers of tyrosine radicals.

CHAPTER I

LITERATURE REVIEW

1.1 Polyphenols

Polyphenols are the second most abundant class of substances in the plant kingdom with more than 8000 phenolic structures currently known (Daayf and Lattanzio, 2008). They are products of plant secondary metabolism and embrace a considerable range of substances that possess an aromatic ring bearing one or more hydroxyl groups. Their structure varies from simple molecules (phenolic acids) to highly polymerized compounds (tannins) (Urquiaga and Leighton, 2000).

Polyphenols are divided into several classes according to the number of phenol rings that they contain and to the structural elements that bind these rings to one another. The main groups of polyphenols are: flavonoids, phenolic acids, phenolic alcohols, stilbenes and lignans (**Figure1**).

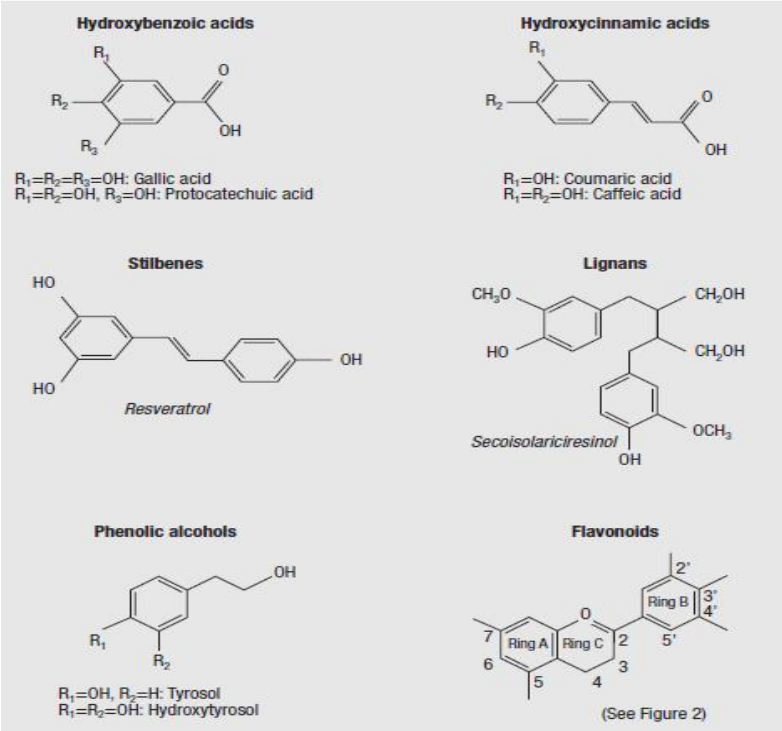

Figure 1: Chemical structure of polyphenols (D'Archivio et al., 2007).

They are highly present in food grains such as sorghum, millet, barley, dry beans, peas, pigeon peas, winged beans, and other legumes; fruits such as apples, blackberries, cranberries, grapes, peaches, pears, plums, raspberries, and strawberries; and vegetables such as cabbage, celery, onion and parsley also contain a large quantity of polyphenols (phenolic compounds are also highly present in tea and wine). Forages such as crown vetch, lespedeza, lotus, sainfoin, and trefoil are also reported to contain polyphenolic compounds (Balasundram et *al.*, 2006).

Polphenols exhibit a wide range of biological effects as a consequence of their beneficial antioxidant properties that can scavenge harmful active oxygen species including $O^{\bullet-}_2$, H_2O_2, $^{\bullet}OH$ and $^1O_2$ (Sakihama et *al.*, 2002). They are important compounds due to their contribution to human health, such as antioxidant activity, antimutagenic and/or anticarcinogenic activities and anti-inflammatory action (Hijova, 2006).

1.1.1 Flavonoids

Flavonoids represent the most common and widely distributed group of plant phenolics (Urquiaga and Leighton, 2000). They share a common carbon skeleton of diphenyl propanes (**Fiure2**); two benzene rings (ring A and B) joined by a linear three-carbon chain.

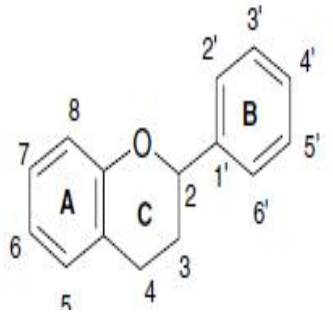

Figure 2: Generic structure of flavonoids (Balasundram et al., 2006).

The central three-carbon chain may form a closed pyran ring (ring C) with one of the benzene rings (D'Archivio et *al.*, 2007) leading to an ideal structural chemistry for free radical scavenging activities and to be more effective antioxidant *in vitro* than vitamins E and C, in addition to their antithrombotic and anti-inflammatory effect (Benkeblia, 2005).

Flavonoids are themselves divided into 6 subclasses, depending on the oxidation state of the central pyran ring: flavonols, flavones, flavanones, isoflavones, anthocyanidins and flavanols (catechins and proanthocyanidins) (**Figure 3**).

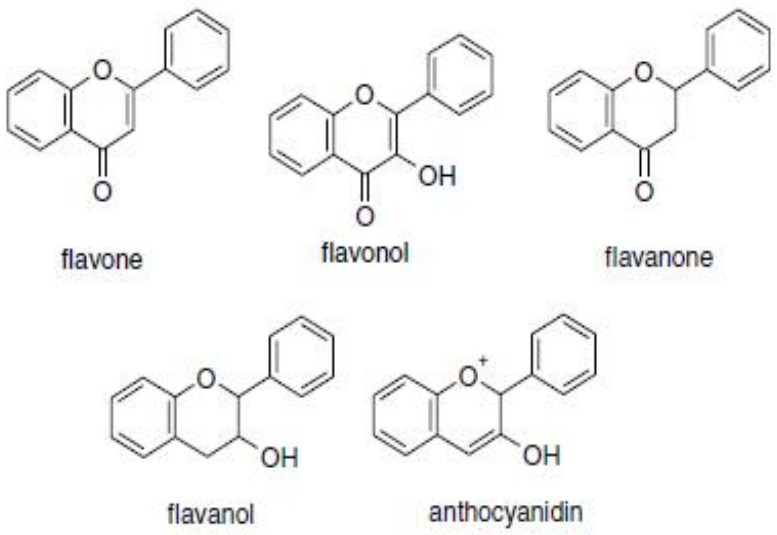

Figure 3: Chemical structure of major classes of flavonoids (Balasundram et al., 2006).

More than 4000 flavonoids have been identified in plants, and the list is constantly growing. This is because of the occurrence of numerous substitution patterns in which primary substituents (such as the hydroxyl group) can themselves be substituted (*i.e.*, additionally glycosylated or acylated), sometimes yielding highly complex structures (D'Archivio et *al.*, 2007).

Table 1: Bioavailability of polyphenols or polyphenol-containing foods

Polyphenols	Source	Quantity of polyphenol ingested (mg)	Maximum concentration in plasma (⊠M)	Urinary excretion (% of intake)	Ref.
Anthocyanins					
Cyanidine 3-glucoside	Orange juice (1 L)	71 mg Cy-3-glc	0.002		[43]
Malvidin 3-glucoside	Red wine (500 mL)	68 mg Mal-3-glc	0.001	0.016 6h	[132]
Malvidin 3-glucoside	Red grape juice (500 mL)	117 mg Mal-3-glc	0.003	0.019 6h	[132]
Cyanidine 3-glucoside	Red fruit extract (1.6 g)	2.7 mg Cy-3-glc/kg bw	0.03		[133]
Flavanols					
Epigallocatechin gallate	Green tea infusion (5 g)	105 mg	0.13-0.31		[130]
Catechin	Red wine (120 mL)	34 mg	0.072		[134]
Epicatechin	Chocolate (80 g)	137 mg	0.26		[135]
Catechin	Pure compound	0.36 mg/kg bw	0.14-0.49	1.2-3	[136]
Epigallocatechin gallate	Pure compound	50-1600 mg	0.28-7.4		[137]
Epigallocatechin gallate	Green tea extract	110-328 mg	0.26-0.7		[138]
Catechins	Black tea	140 mg	0.34		[139]
Procyanidin B1	Grapeseed extract	18 mg	0.011		[140]
Flavanones					
Hesperidin	Orange juice	61 mg	0.48	4.1	[141]
Hesperetin	Orange juice	110-220 mg	0.46-1.28	4.1-6.4	[123]
Naringenin	Orange juice	22.6-45 mg	0.06-0.2	7.1-7.8	[123]
Naringenin	Grapefruit juice	199 mg	5.99	30.2	[142]
Naringenin	Pure compound	135 mg	7.4	5.8	[143]
Hesperetin	Pure compound	135 mg	2.7	3.3	[143]
Flavonols					
Quercetin	Apples	107 mg	0.3	3.5	[131]
Quercetin	Onions	100 mg	7.6	6.4	[83]
Quercetin 4'-glucoside	Pure compound	100 mg	7.0	4.5	[83]
Quercetin	Buckwheat tea	200 mg	2.1	1.0	[83]
Quercetin	Pure rutin	200 mg	1.1	0.9	[83]
Isoflavones					
Daidzein	Soy milk	108 mg	0.47	37.3	[144]
Genistein	Soy milk	102 mg	0.41	20.2	[144]
Glycitein	Soy milk	114 mg	0.09		[144]
Daidzein	Pure compound	50 mg	0.76		[121]
Genistein	Pure compound	50 mg	1.26		[121]
Glycitein	Pure compound	25 mg	0.72		[121]
Daidzein	Soy extract	0.28-0.84 mg/kg bw	1.7-9.0	26-42	[145]
Genistein	Soy extract	2-16 mg/kg bw	3.4-25.4	9.5-14	[145]
Daidzein	Soy nuts	6.6-26.4 mg	0.4-1.65	63-44	[146]
Genistein	Soy nuts	9.8-39.2 mg	0.59-2.21	25.2-15.8	[146]
Hydroxybenzoic acids					
Gallic acid	Pure compound	50 mg	1.8GA+2.3 MeGA		[147]
Gallic acid	Assam black tea	50 mg	1.8GA+2.3 MeGA	36.4	[147]
Gallic acid	Red wine (300 mL)	4 mg	1.8GA+2.3 MeGA	39.6	[148]
Hydroxycinnamic acids					
Chlorogenic acid	Coffee (200 mL)	96 mg	0.5 caffeic acid		[149]
Caffeic acid	Red wine (200 mL)	1.8 mg	0.06		[150]
Caffeic acid	Red wine	0.06 mg	0.08		[151]
Hydrocinnamic acids	Apple cider (1.1 L)	15 mg	0.43		[152]

GA: gallic acid; MeGA: methylgallic acid; bw: body weight.

(Source: D'Archivio et *al.*, 2007)

1.1.2 Chalcones

Chalcones constitute minor family of substances belonging to the flavonoids. They are highly reactive substances of a varied nature and they experience chemical and physical transformations of great importance in different experimental models (Gasull et *al*., 2005). Chalcones belong to a class of α, β-unsaturated aromatic ketones (**Figure 4**) responsible for the antimicrobial activity, which occurs abundantly in nature, especially in plants.

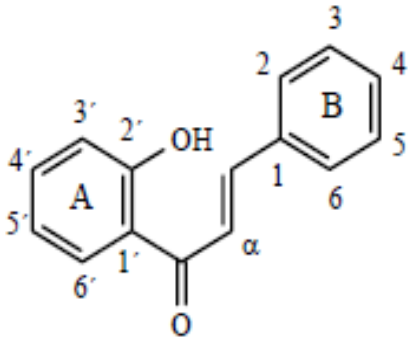

Figure 4: Structure of chalcones (Valisek et al., 2008).

Chalcones are promising and interesting compounds due to their vast applications in the pharmaceutical and agricultural industry (Correa et *al.*, 2008). They are well known as intermediates for the synthesis of various heterocyclic compounds (Prasad et *al*., 2008). They are also the biosynthetic precursors of the major flavonoids (Abe et *al*., 2005). The compounds with the backbone of chalcones have been reported to possess remarkable biological activities due to their intervention as antimicrobial, anti-inflammatory, analgesic, antiplatelet, antiulcerative, antimalarial, anticancer, antiviral, antileishmanial, antioxidant, antitubercular, antihyperglycemic and immunomodulatory agents, as well as being inhibitory of chemical mediator release, leukotriene B, tyrosinase and aldose reductase activity (Prasad et *al.*, 2008).

1.1.3 Chalcone synthesis

Chalcones are called “anthochlor pigments”, coined to identify a group of yellow pigments that turn red in the presence of alkali (Yoichi et *al.*, 2005). The chalcone synthases CHS (EC:2.3.1.74) superfamily of type III polyketide synthases are pivotal enzymes in the biosynthesis of flavonoids as well as of a variety of structurally diverse plant secondary metabolites with remarkable biological activities (stilbenes, benzophenones, pyrones, chromones, acrydones, phloroglucinols and resorcinol) (Abe et *al*., 2005). Peter et *al*. (1986) showed that this synthesis is involved in pigment formation, symbiosis and plant defence against pathogen attack and exposure to UV light (Contessotto et *al*., 2001).

Chalcone synthase catalyses the sequential, decarboxylative addition of three acetate units from malonyl-CoA to a hydroxycinnamoyl-CoA as a starting precursor, followed by cyclization to produce THC (**Figure 5**) (Masayoshi et *al*. 2006), which undergoes a rapid spontaneous isomerization to naringenin-chalcone, leading to the formation of flavanols, flavanones, isoflavanoids and anthocyanins (Contessotto et *al.*, 2001).

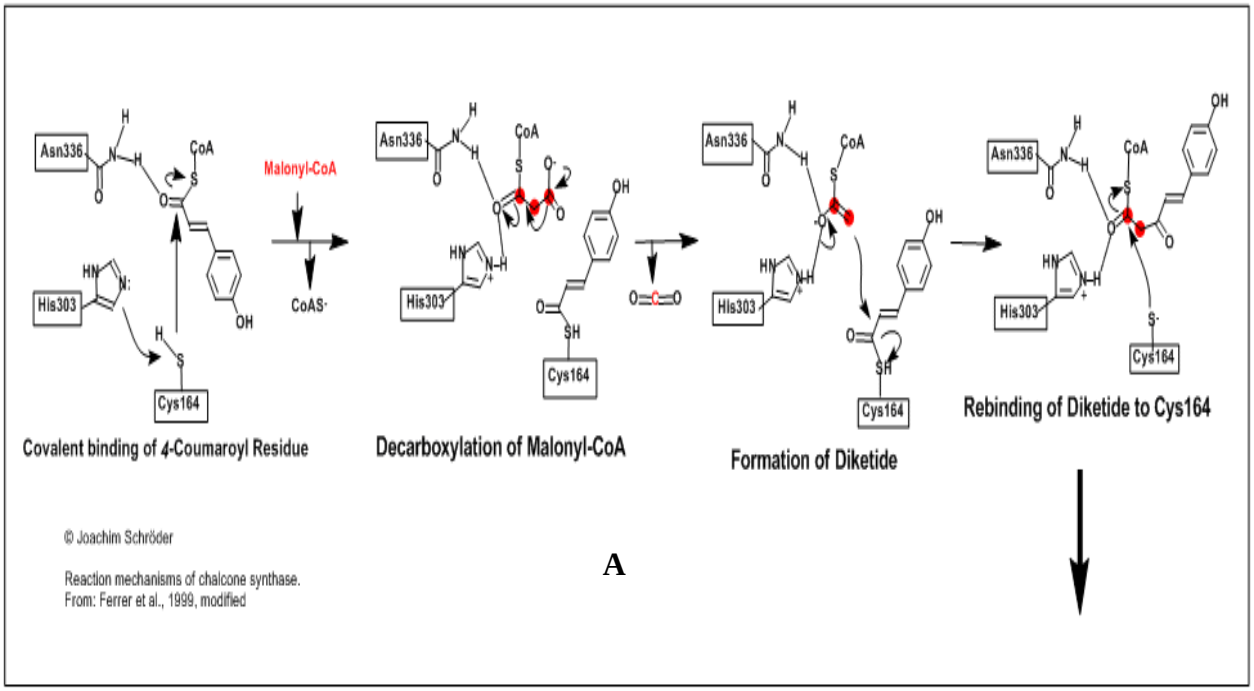

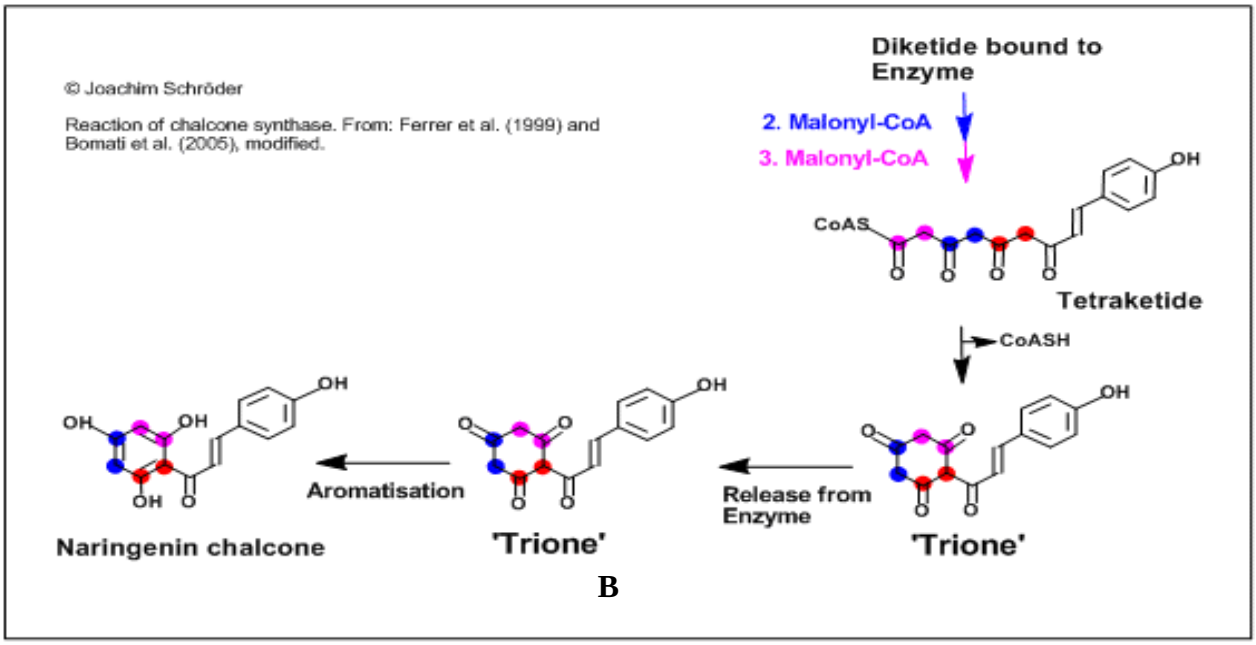

Figure 5: Chalcone synthase catalyzed condensation reaction (A) and condensation ring closure and aromatization (B) (Ferrer et al., 1999).

Chalcone synthase could also utilize caffeoyl-CoA as a starting ester to produce PHC. In most plant species *p*-coumaroyl-CoA serves as the precursor of 2',4',4',6'-tetrahydroxychalcone, a pivotal precursor of a diverse group of flavonoids. When caffeoyl-CoA is used as a precursor only a small amount of 4'-*O*-glugosides of THC and 2',3,4,4',6'-pentahydroxychalcone have been identified in yellow flowers of snapdragon (*Antirrhinum majus)*. Recent studies suggest that chalcone glycosides serve as direct precursors of aurones, which are mainly responsible for the yellow colour of flowers (Masayoshi et *al.* 2006).

Phytoalexins, plant defence substances, are derived from the flavonoid pathway and they are used as markers in the detection of plant infection by microorganisms by checking the accumulation of chalcone synthase mRNA or by measuring the activity of this enzyme (Contessotto et *al.*, 2001).

1.1.4 Aurones

The term "aurone" comes from Latin meaning "aurum or gold" because of the golden yellow colour of the pigments. Aurones are plant flavonoids that provide a yellow flower colour to a variety of popular ornamental flowers such as snapdragon, cosmos, and dahlia (Toru et *al.*, 2001). Aurones are 2-benzylidene-coumaran-3-ones with multiple hydroxyl (or *O*-substituted hydroxyl) functions in their aromatic rings (**Figure 6**) (Toru, 2002).

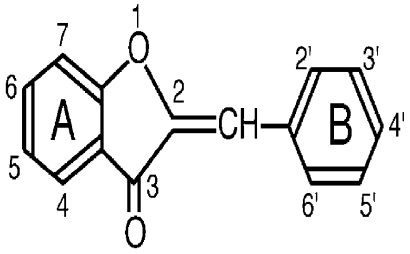

Figure 6: Chemical structure of aurones (Toru, 2002).

In addition to their pigmentation role, aurones are described as phytoalexins, used by plants as defence against various infections. They have remarkable properties exhibiting antiviral, antiparasitic, antifungal, and antidiabetic activities (Somepalli et *al.*, 2007).

It has been suggested that their biosynthesis is closely related to that of chalcones. They are categorised into a class of flavonoids called "anthochlor pigments", but a detailed biosynthetic pathway remained unknown since their discovery nearly 50 years ago (Sato et *al.*, 2001). In 2000 the biosynthetic pathway of aurones from chalcones in yellow snapdragon was established by Toru et *al.* (2001)**.** Aurones are generally prepared by two main methods: condensation between benzofuranones and benzaldehydes in the presence of acidic or basic reagents or neutral alumina (chemical synthesis), and by oxidative cyclisation of 2'-hydroxychalcone (natural synthesis) (Venkateswarlu et *al.*, 2007).

1.1.5 Aurone synthase

Aureusidin synthase is a binuclear copper enzyme with sugar chain(s) and was identified as a homologue of plant polyphenol oxidase (PPO). It is established that the biosynthetic pathway of aurones from chalcones in yellow snapdragon flowers is catalyzed by aureusidin synthase, with dual chemical transformations: first 3-hydroxylation and second oxidative cyclisation (2', α-dehydrogenation) of 2', 4, 4', 6'-tetrahydroxychalcone (THC) to produce aureusidin (Toru et *al*., 2001) (**Figure 7**).

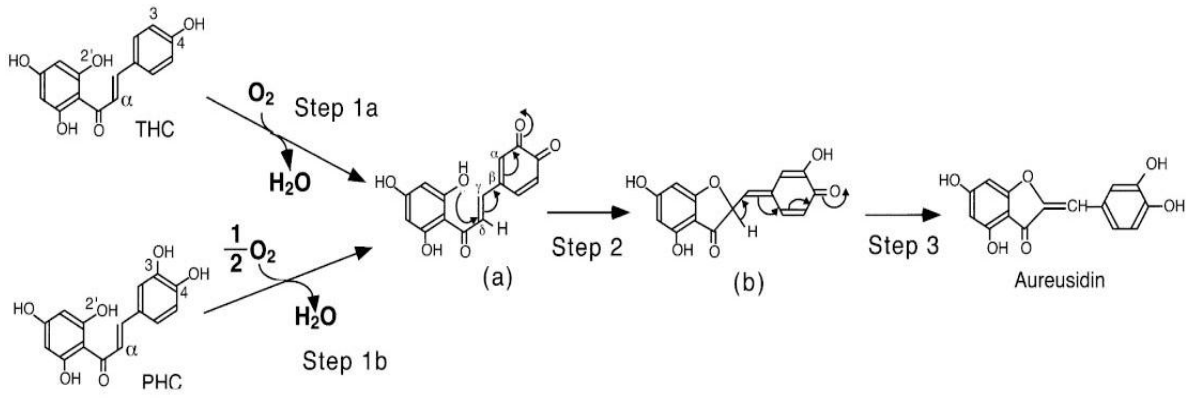

Figure 7: Mechanism of aurone synthesis from THC and PHC catalyzed by aureusidin synthase (Toru, 2002).

1.2 Peroxidases

Peroxidases are known to occur in different tissues and the pattern of expression and properties of these peroxidases vary between them. Peroxidases are iron haem-containing oxidoreductases (EC 1.11.1.7) that reduce peroxides, mainly hydrogen peroxide, to water and subsequently oxidize small molecules, often aromatic oxygen donors (Delannoy et *al.*, 2006). They are ubiquitous in nature and are involved in various physiological processes in plants. Studies have suggested that peroxidases play a role in lignification, suberization, cross-linking of cell wall structural proteins, auxin catabolism, self-defence against pathogens and senescence (Hiraga et *al.*, 2001).

Plant peroxidases contain two-calcium ions (Ca^{2+}), which are very essential for the structural stability and thermal stability of the enzyme as well as its *in vitro* activation during analysis (Manu and Prasada Rao, 2009 and Sticher et *al.*, 1981). Peroxidases are widely used in clinical laboratories and industries as well as their application in environmental conservation (Lopez-Molina et *al.*, 2003).

1.2.1 Catalytic cycle of peroxidase

During the catalytic cycle of peroxidase, the ground state enzyme undergoes a two-electron oxidation by H_2O_2 forming an intermediate state called compound I (E). Compound I (E) will accept an aromatic compound (AH_2) in its active site and will carry out its one-electron oxidation, liberating a free radical ($^{\bullet}AH$) that is released back into the solution, and converting to compound II (Ei). A second aromatic compound (AH_2) is accepted in the active site of compound II (Ei) and is oxidised, resulting in the release of a second free radical ($^{\bullet}AH$) and the return of the enzyme to its resting state, completing the catalytic cycle (**Figure 8**). The two free radicals ($^{\bullet}AH$) released into the solution combine to produce insoluble precipitate that can easily be removed by sedimentation or filtration.

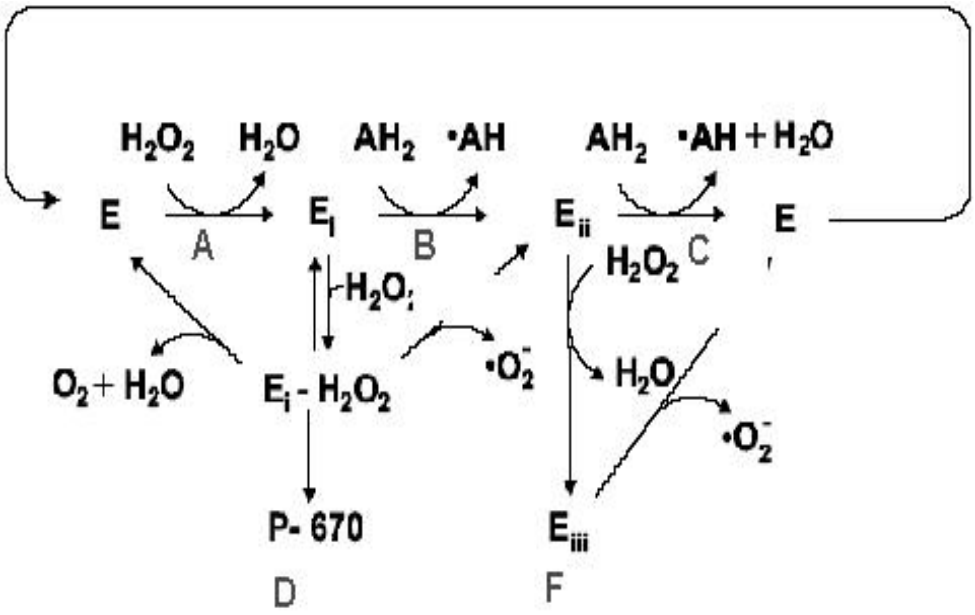

Figure 8: Complete peroxidases catalytic cycle (Villalobos and Buchanan, 2002).

The stoichiometry reported, based on one mole of peroxidase consumed per mole of aromatic compound removed from the solution, this stoichiometry depends also on the amount of enzyme consumed in side reaction and the precipitating oligomers. Therefore, it is very close to one.

Various side reactions that take place during the removal process are responsible for the enzyme inactivation (E) or inhibition (Eii) leading to a limited lifetime, but this form is not permanent since compound III (Eii) decomposes back to the resting state of peroxidase.

Some peroxidases, like horse radish peroxidase (HRP), lead to a permanent inactivation state (P-670) when H_2O_2 is present in excess or when the end-product polymer adheres to its active site, causing its permanent inactivation by causing changes in its geometric configuration (Villalobos and Buchanan, 2002).

The optimisation of enzymic activity is very important for related applications. Response Surface Methodology, as succinctly described below, is a useful tool for this purpose.

1.2.2 Response Surface Methodology

As an important subject in the statistical design of experiments, the Response Surface Methodology is a collection of mathematical and statistical techniques useful for modelling, formulating, developing and analyzing as well as also being efficient in the improvement of existing studies and products in which a response of interest is influenced by several variables; the objective is to optimize this response (Bradly, 2007). This technique was introduced in the early 50's by Box and Wilson (1951) but only recently has there been interest in applying RSM to Clinical and Biological laboratory assay design, to Industrial routine assay design, to Social Science, to Food Science, to Physical and Engineering Science and to several national and international standardization committees that are using RSM as a tool for the development of reference methods (London et *al.*, 1982).

When there is a curvature in the response surface the first-order model is insufficient, so the second-order model is useful in approximating a portion of the true response surface with parabolic curvature (Bradly, 2007) that can be represented graphically, either in the three-dimensional space or as *contour plots* that help visualise the shape of the response surface; hills, valleys and ridge lines (**Figure 9**).

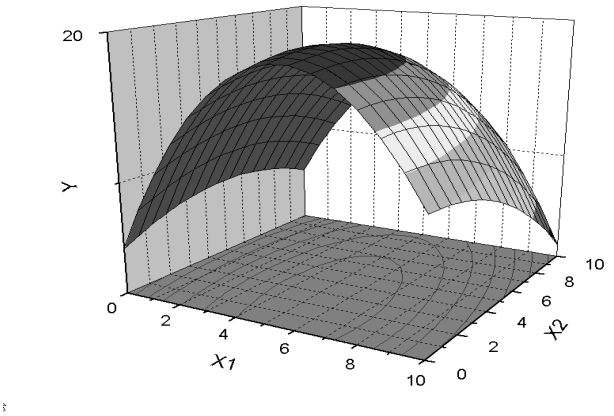

Figure 9: Example of a response (Jimenez-Contreras, 2009).

Generally, Response Surface Methodology has been developed for the following purposes:

- Understanding the topogrphy of the response surface (local maximum, local minimum, ridge lines).

- Finding the region where the optimal response occurs. The goal is to move rapidly and efficiently along a path to get to a maximum or a minimum response so that the response is optimised (Bradly, 2007).

1.2.3 Different classes of peroxidases

Peroxidases, a class of enzymes in animal, plant and microorganism tissues, catalyze oxidoreduction between H_2O_2 and various reductants. Peroxidases fall into two major superfamilies according to their primary sequence: animal and plant peroxidases (**Table 2**).

Table 2: Classification of peroxidases

Superfamily	Class[a]	Member (EC number)	Origin	Molecular weight (kDa)
Animal peroxidase		Eosinophill peroxidase (EC 1.11.1.7)	Animal	50–75
		Lactoperoxidase (EC 1.11.1.7)	Animal	78–85
		Myeloperoxidase (EC 1.11.1.7)	Animal	79–150
		Thyroid peroxidase (EC 1.11.1.7)	Animal	90–110
		Glutathione peroxidase (EC1.11.1.9)	Animal and plant	6–22 and 75–112 [b]
		Prostaglandin endoperoxide synthase (EC 1.14.99.1, partial) [c]	Animal	115–140
Catalase		Catalase (EC 1.11.1.6)	Animal, plant, fungus and yeast	140–530
Plant peroxidase	I	Cytochrome *c* peroxidase (EC 1.11.1.5)	Yeast and bacterium	32–63
		Catalase-peroxidase (EC 1.11.1.6)	Bacterium and fungus	150–240
		Ascorbate peroxidase (EC1.11.1.11)	Plant	30–58
	II	Manganese-dependent peroxidase (EC 1.11.1.13)	Fungus	43–49
		Ligninase (EC 1.11.1.14)	Fungus	40–43
	III	Peroxidase (EC 1.11.17, POX)	Plant	28–60

[a] Established only for the plant peroxidase superfamily.
[b] Molecular weights for monomeric and tetrameric forms, respectively.
[c] Homology was observed in the central region (approximately 180 residues) with other animal peroxidases.
(Hiraga et *al.*, 2001)

1.2.4 Plant peroxidases

Based on differences in primary structure, the plant peroxidase superfamily can be further divided into three classes (**Table 2**). Class I contains intracellular peroxidases related to bacterial peroxidases, such as ascorbate peroxidases or bacterial catalase-peroxidases or the cytochrome c peroxidase of *Saccharomyces cerevisiae*. Class II contains fungal-secreted peroxidases, i.e. lignin peroxidases or manganese peroxidases, and class III peroxidases are of plant origin (Delannoy et *al.*, 2006).

1.2.5 Peroxidase function overview

1.2.5.1 In plant

Plant peroxidases have often been suggested to be involved in the biosynthesis of complex cell wall macromolecules such as lignin and suberin, which are synthesized by plant for mechanical strength, defence, restoring damaged tissues, and water transport (Vidali, 2001 and De Gara, 2004*).*

Plant PODs oxidise phenolic domains of feruloylated polysaccharides and tyrosine residues of cell wall structural proteins such as hydroxyproline-rich glycoproteins to form more complex and larger molecules in the cell wall, thereby restricting cell expansion and pathogen invasion. In tobacco, a positive correlation was found between POXs activity and resistance to tobacco wildfire disease. The roles of POXs in defence are considered as follows:

- Reinforcement of cell wall physical barriers comprising lignin, suberin, feruloylated polysaccharides and hydroxyproline-rich glycoproteins,
- Enhancement of reactive oxygen species production as signal mediators and antimicrobial agents,
- Enhancement of phytoalexin production.

Generally, multiple POXs are induced by pathogen infection, suggesting that each POX is involved in a specific defence process (Hiraga et *al.***,** 2001 and Cosio and Dunand, 2009).

Peroxidases from tobacco and HRP have showed higher specific activities to NADH, NADPH and IAA than to monolignols, suggesting their involvement in some cell wall biosynthetic processes other than polymerization of monolignols (**Figure 10**) (Delannoy et al., 2006 and Cosio and Dunand, 2009).

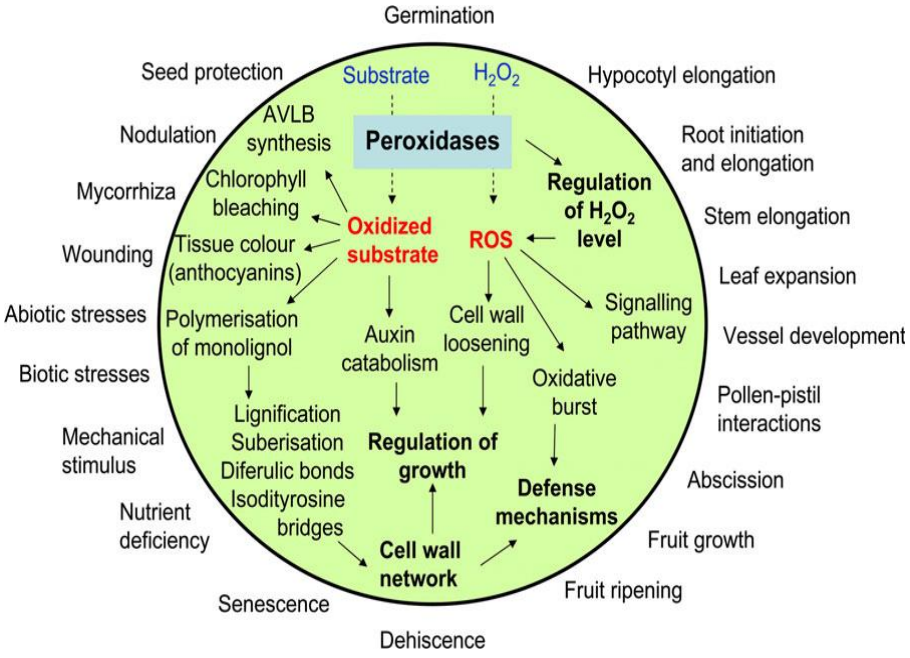

Figure 10: The diverse functions and roles of class III peroxidases (Cosio and Dunand, 2009).

1.2.5.2 In pharmacology and fine chemistry

Recently, peroxidases have been used as reagents for organic synthesis and biotransformations, as well as in coupled enzyme assays, chemiluminescent assays, immunoassays and for the treatment of waste waters. *In vitro* sustainable results regard peroxidase mechanisms have been reported such as:

- Oxidative decarboxylation of Auxin (IAA). A plant hormone that affects many physiological processes by POXs (from tobacco and HRP). POXs induce IAA inactivation, thereby offering new potential for target cancer therapy. Studies reported

that IAA is cytotoxic to human tumour cells in the presence of POD. The mechanism of toxicity involves 3-methylene-2-oxindole which is generated through IAA oxidation.

- Some applications of HRP in small-scale organic synthesis include N- and O-dealkylation, oxidative coupling, selective hydroxylation and oxygen-transfer reactions:

    - Peroxidase-catalysed oxidative coupling of methyl-(E)-sinapate with the syringyl lignin-model compound, 1-(4-hydroxy-3,5-dimethoxyphenyl) ethanol yielded a novel spirocyclohexadienone together with a dimerization side-product.
    - Coupling of catharanthine and vindoline to yield α-3′,4′-anhydrovinblastine. This reaction, catalysed by HRP, offers potential interest as it is a semisynthetic step in the production of the anti-cancer drugs vinblastine and vincristine from *Catharanthus roseus* (Vidali, 2001 and Veitch, 2004).

- Peroxidases have also shown an action on tyrosine, both as free amino acid and in peptides or proteins. After one electron oxidation and subsequent deprotonation, dityrosines and higher oligomers are produced.
- Ferulic acid and tyrosine are subject to peroxidase-mediated oligomerization. Such peroxidase-mediated hetero-coupling could provide an explanation for the occurrence of protein-carbohydrate complexes in plant cell walls and the incorporation of ferulic acid and other hydroxycinnamic derivatives into lignin and suberin tissues on a protein template. Recent studies have further explored the mechanism of hetero-adduct formation of GYG (Gly-Tyr-Gly) and FA. (Ahn et *al*., 2002).
- Reactive oxygen species (ROS) generated through abiotic and biotic stresses trigger programmed cell death (PCD) in mammalian cells, yeast and plants (Delannoy, 2005). In plants and yeast the PCD is induced by Bax proteins that cause organelle dysfunction by their localisation onto the outer mitochondrial membranes and formation of ion channels. Several enzymes have been reported to suppress Bax-induced cell death such as peroxidase, ascorbate peroxidase, peroxidase with glutathione transferase and phospholipid hydroperoxid glutathione peroxidase (Chen et *al.*, 2004; De Gara, 2005).

- Many studies have suggested an association of plant peroxidases with production and scavenging of hydrogen peroxide, porphyrin metabolism, senescence and organogenesis, indicating that POXs have diverse functions (Hiraga et *al.*, 2001).

Based on previous published works (El Agha et *al.* 2008; 2009; Osman et *al.*; 2008; Majdalany, 2008) for the exploitation and valorisation of crude POD from cheap onion waste sources, the present thesis is a further insight into the enzyme properties leading to green and cheap synthetic applications for fine chemicals: the case of chalcone syclisation into aurones. Pentahydroxy and dihydroxy chalcones are the studied substrates.

CHAPTER II

MATERIALS AND METHODS

2.1 Chemicals and reagents

- 4-AAP (4-aminoantipyrine), Sigma-Aldrich
- Acetone, Fluka
- Anhydrous K_2CO_3, Riedel de Haên
- Boric acid (H_3BO_3), Applichem
- Calcium chloride, Merck
- Celite 545, Sigma
- Charcoal activated pure, Merck
- Citric acid monohydrate, Merck
- Disodium hydrogen phosphate dihydrate, Merck
- DMF (N-N dimethylformamide), Fluka
- Ethanol, Sigma-Aldrich
- Ethyl acetate, Merck
- Hydrochloric acid (37%), Riedel-de Haën
- Hydrogen peroxide (30%), Merck
- Methanol, Sigma-Aldrich
- Potassium chloride, Merck
- Potassium dihydrogen phosphate, Merck
- Protocatechuic acid, Sigma-Aldrich
- PVPP (polyvinylpyrrolidine), Sigma-Aldrich
- Sodium hydroxide, Merck
- Sodium sulfate anhydrous, Sigma-Aldrich
- TCA (Trichloroacetic acid), Sigma-Aldrich

2.2 Apparatus

- Balance, Mettler AT 261 Deltarange
- Balance, Mettler PM 2000
- Centrifuge, MLW T 23 D
- Micro-centrifuge, biofuge pico, Heraeus

- LC-DAD- MS setup consisting of:
  - System P4000 LC pump (Finnigan);
  - System UV 6000 LP diode array detector (Finnigan);
  - System P4000 (TSP) autosampler;

2.3 Preparation of the onion solid waste homogenate

10 g onion solid waste (the apical trimmings) were dispersed in 100 mL phosphate buffer pH4 (phosphate buffer containing 0.1M citric acid and 0.2 M disodium hydrogen phosphate) mixed with 5g PVPP and were ground in a domestic blender. Then the mix was centrifuged at 3000 rpm for 15 min. Following this, the supernatant was filtered through filter paper to achieve transparency. The clear filtrate was used as the crude enzyme source.

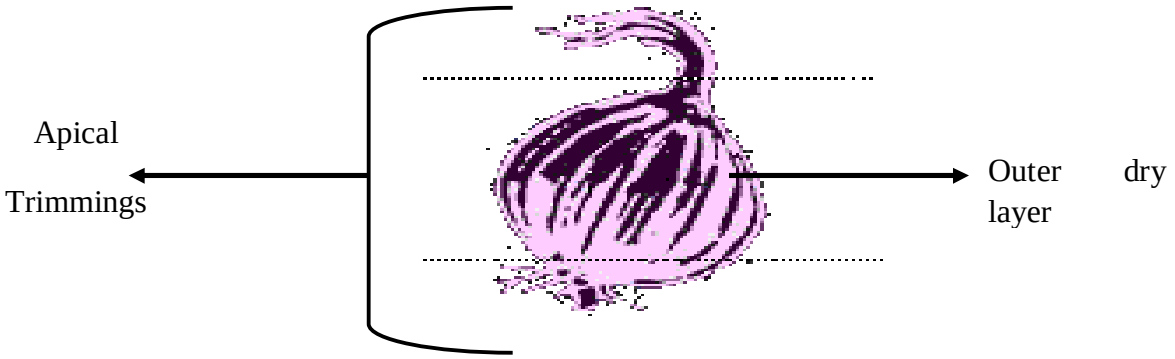

Figure 11: Parts of onion bulb used as the enzyme homogenate source

2.4 Determination of the optimum conditions for enzymic activity

2.4.1 Onion POD optimization using protocatechuic acid as a substrate

2.4.1.1 Effect of temperature

The temperatures tested values of 5, 20, 30, 40, 50, 60 and 70º C.

The final curve for the estimation of the optimum temperature was obtained by measuring the reaction at different temperature values. The slope of the curve obtained for every point was taken to obtain a final curve with the equation $\Delta A_{510}=f(T)$ from which the optimum temperature was estimated. From a similar principle the optimum of each parameter was estimated.

2.4.1.2 Effect of pH

The pH tested values were 2, 3, 4, 5, 6, 7, and 8. For a pH range from 3 to 7 a phosphate buffer was used. For pH=2 a potassium chloride buffer (containing 0.2M KCl and 0.2M HCl) was used. For pH=8 a boric acid buffer (containing 0.1M of both KCl and H_3BO_3) was used.

2.4.1.3 Effect of H_2O_2 concentration

Different concentrations of H_2O_2 solution were tested to determine the optimum concentration. The tested concentration values were: 0.005, 0.01, 0.02, 0.05, 0.08, 0.1, 0.15, 0.2, 0.3, 0.4, 0.5, 0.7, 0.8, 1.0, 1.2, 1.5 and 2 mM.

All H_2O_2 solutions were prepared by dissolving H_2O_2 in a phosphate buffer solution at pH 6.

2.4.1.4 Effect of substrate concentration

Different concentrations of the substrate were prepared to determine the optimum concentration. The tested values were: 0.1, 0.2, 0.3, 0.5, 0.8, 1.0, 1.5, 2.0, 2.5, 3.0, 4.0 and 5.0mM.

The substrate solutions were prepared by dissolving the exact amount of the phenolic acid in DMF.

2.4.1.5 Effect of enzyme dilution

Different onion POD extract dilutions were prepared to determine the optimum concentration of the crude enzyme extract:

The crude onion POD extract dilutions prepared varied between 0.1, 0.2, 0.3, 0.5, 0.8 and 1 from the initial onion POD extract fraction.

The crude enzyme solutions were prepared by dissolving the exact amount of the enzyme in buffer solution pH 6.

2.4.1.6 Determination of the reaction rate

An aliquot of 0.25ml of 4-AAP (10mM in H_2O) was mixed with 0.1ml PA (100mM in DMF), 0.1ml H_2O_2 (2mM in phosphate buffer pH6), 0.5ml buffer pH6 and 0.1 ml of the crude onion POD extract, and then the absorbance at 510 nm was measured every 10 sec up to 2 min. One enzyme unit was defined as ΔA_{510}nm per sec.

Control samples were prepared by replacing the enzyme extract with the buffer solution.

All the experiments were done in triplicate.

2.4.1.7 Treatment of the phenolic substrates with onion POD extract

After the determination of the optimum conditions for each case, the final reaction of each substrate with onion POD extract was carried out using a reaction medium of 1 mL, which consisted of 0.1 mL of the onion POD extract at pH4, 0.1 mL of substrate (PA) solution 2 mM in DMF, and 0.8 mL H_2O_2 (0.8 mM in phosphate buffer solution at the selected pH of the reaction pH6). The reaction medium was then incubated for 10 min, 30min and 3 hours at the optimum temperature (30°C), and then 0.1 mL of 10% TCA solution in ethanol was added to stop the reaction. The reaction medium was centrifuged at 5000rpm for 10 minutes. The resulting solution was kept in the freezer for further analysis.

2.4.1.8 LC-DAD-MS analysis

For the reaction of the crude POD extract with simple phenolics (protocatechuic acid) the analysis was performed using an LC/DAD/MS system comprising a Finnigan MAT Spectra System P4000 pump coupled with a UV6000LP diode array detector and a Finnigan AQA mass spectrometer. The separation was performed on a 125 x 2 mm Superspher 100-4 RP-18 column (Macherey-Nagel, 4μ particle size) at a flow rate of 0.33 ml/min, the column being kept at 40^0C. The detection was monitored at 278 and 340 nm. For the MS-ESI (+) spectroscopy the probe temperature was 350 $^{\circ}$C, the probe voltage 4 kV and the collision induced fragmentation energies 12 and 50 eV (CID) in the mass analyzer. The mass range was set at 121-787 amu and the scan rate was at 0.8 scans/sec. The following gradient program was used: (A)

AcOH and (B) MeOH, 2.5%. The flow rate was 0.33 mL min^{-1} and the elution programme was: 0-5 min, 0% B; 5-30 min, 100% B; 30-35 min, 100% B. The data were processed using the Xcalibur 1.2 software.

2.4.2 Onion POD enzymic activity optimization using pentahydroxy chalcone as substrate

2.4.2.1 POD activity by the response surface methodology technique

2.4.2.1.1 Chalcone reaction with onion POD

In order to determine the optimum conditions, the reaction was carried out by mixing 0.1 ml of crude POD extract solution (in phosphate buffer, pH4), 0.1 ml of 1.72 mM chalcone solution in DMF and 0.8 ml H_2O_2 (3 mM in a buffer solution at pH 3, 5 and 7). The reaction medium was incubated for 1, 3 and 5 hours at 20, 30 and 40°C. Then 0.1 ml of TCA solution in 10% ethanol was added to stop the reaction. The reaction medium was centrifuged at 5000rpm for 10 minutes. The resulting solution was kept in the freezer.

2.4.2.1.2 Experimental design

A 2^3 full-factorial experimental design was used to identify the relationship between the response function and the process variables, as well as to determine the conditions that optimized the cyclization process. The three independent variables or factors studied were temperature (X_1, which varied between 20 and 40°C); pH (X_2, which varied between 5 and 7) and reaction time (X_3, which varied between 1 and 5h). Each variable to be optimized was coded at three levels, -1, 0 and 1 (see **Table3)**.

Table 3: Experimental values and coded levels of the independent variables used for the 2^3 full-factorial design

Independent variables	**Code units**	**Coded variable level**		
		-1	**0**	**1**
T (C)	X_1	20	30	40
pH	X_2	5	6	7
Time (h)	X_3	1	3	5

The three independent variables were coded according to the following equation:

$$x_i = \frac{Xi - X0}{\Delta Xi}, \qquad x_i = 1, 2, 3$$

Where:

x_i and X_i are the dimensionless and the actual value of the independent variable i, X_0 is the actual value of the independent variable i at the central point, and ΔX_i is the step change in X_i corresponding to a unit change in the dimensionless value.

Response (aureusidin peak area) at each design point was recorded (**Table 2**). Data from the central composite experimental design were subjected to regression analysis using least square regression methodology to obtain the parameters of the mathematical models. The Student's *t*-test permitted to check the statistical significance of the regression coefficients (**Table 3**) deriving from the model. Analysis of variance (ANOVA) was applied to evaluate the statistical significance of the model. Surface plots that show the response as a function of the simultaneous variation of the independent variable were obtained using the fitted model. Response surface plots (**Figure 18, 19 and 20**) were obtained using the fitted model, by keeping the independent variable simultaneous (Kiassos et *al.*, 2009; Mylonaki et *al.*; 2008 and Chan et *al.*, 2009).

2.4.2.1.3 LC-DAD-MS analysis

For the reaction of chalcone cyclisation to the aurone scaffold, the analysis was performed using an LC/DAD/MS system comprising a Finnigan MAT Spectra System P4000 pump coupled with a UV6000LP diode array detector and a Finnigan AQA mass spectrometer. The separation was performed on a 125 x 2 mm Superspher 100-4 RP-18 column (Macherey-Nagel, 4µ particle size) at a flow rate of 0.33 ml/min, the column being kept at 40°C. The detection was monitored at 370, 400 and 278 nm. For the MS-ESI(+) spectroscopy the probe temperature was 350 °C, the probe voltage 4 kV and the collision induced fragmentation energies 12 and 40 eV (CID) in the mass analyser. The mass range was set at 121-787 amu and the scan rate was at 0.8 scans/sec. The following gradient program was used: (A) AcOH (2,5%) and (B) MeOH, 100% A for 5 min, 0% A for 15 min and kept at 0% A for another 5 min. The data were processed using the Xcalibur 1.2 software.

2.4.2.1.4 Statistical analysis

All determinations were carried out at least in triplicate and values were averaged and given with the standard deviation (±SD). Linear regression analyses were performed at the 95% significance level. For all statistical work, JMP™5.1 and Microsoft Excel™2000 were used.

2.5 Scale up of the chalcone cyclisation reaction

2.5.1 Scale up of the onion POD reaction with pentahydroxy chalcone

After optimization as mentioned in page 30, 13mg of pentahydroxy chalcone were dissolved in 1ml DMF and added to a mixture containing an aliquot of 19.2 ml H_2O_2 solution (3mM in phosphate buffer pH5) and 2.2 ml crude enzyme extract solution. The final reaction volume is 22.4 ml with a product final concentration of 2mM (optimum substrate concentration for the reaction). The reaction was left to proceed at room temperature between 1.5 and 3h and then stopped by the addition of 2.2ml of TCA (10% in EtOH) and centrifugation at 5000 rpm for10mn. The mixture was extracted with ethyl acetate and the organic layer dried on Na_2SO_4. After vacuum

distillation of the solvent on a rotary evaporator the residue was redissolved in 2ml of methanol and kept in stock.

2.5.2 Scale up reaction with dihydroxy chalcone

13mg of dihydroxy chalcone was dissolved in 1ml DMF and added to a mixture containing an aliquot of 19.2 ml H_2O_2 solution (3mM in phosphate buffer, pH5) and 2.2 ml crude enzyme extract. The final reaction volume was 22.4 ml with a final product concentration of 2mM (optimum substrate concentration for the reaction). The reaction was left to rest at room temperature between 1.5 and 3h and then stopped by the addition of 2.2ml of TCA (10% in EtOH) and centrifugation at 5000 rpm for10min. The mixture was extracted with ethyl acetate and the organic layer dried on Na_2SO_4. After vacuum distillation of the solvent on a rotary evaporator the residue was redissolved in 2ml of methanol and kept in stock.

CHAPTER III

RESULTS AND DISCUSSION

3.1 Biocatalytic properties of onion POD

3.1.1 Optimisation of enzyme activity using protocatechuic acid as substrate

Protocatechuic acid (3, 4-Dihydroxybenzoic acid, PA) was chosen for enzymic reaction optimization in view of studying enzymic activity on a simple dihydroxy phenol structure.

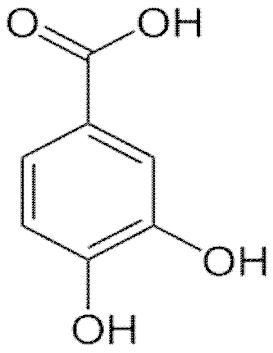

Figure 12: Chemical structure of protocatechuic acid.

Preliminary experiments using quercetin, which is a physiological substrate for onion POD, ferulic acid and cafeic acid showed that maximum activity was attained at pH4 for quercetin and ferulic acid and pH5 for caffeic acid respectively. The optimum concentration of H_2O_2 for the 3 substrates showed maximum activity at 2.4, 1.6 and 0.8 mM respectively (El Agha et *al.*, 2008; 2009 and Osman et *al.*, 2008). For this reason, initial investigations pertaining to the effect of temperature and pH on protocatechuic acid (which is a ferulic acid derivative) oxidation rate where performed at pH4 and $[H_2O_2]$ = 2 mM.

3.1.1.1 Effect of temperature covariance

The reaction rate as a response to temperature change was found to be exponential until an optimum temperature was reached at 30°C. After that the reaction rate decreased dramatically (three-fold) between 30 and 40°C and it continued to decrease, reaching a minimum between 50 and 60°C, whereas it became almost nil between 60 and 70°C (**Figure 13).**

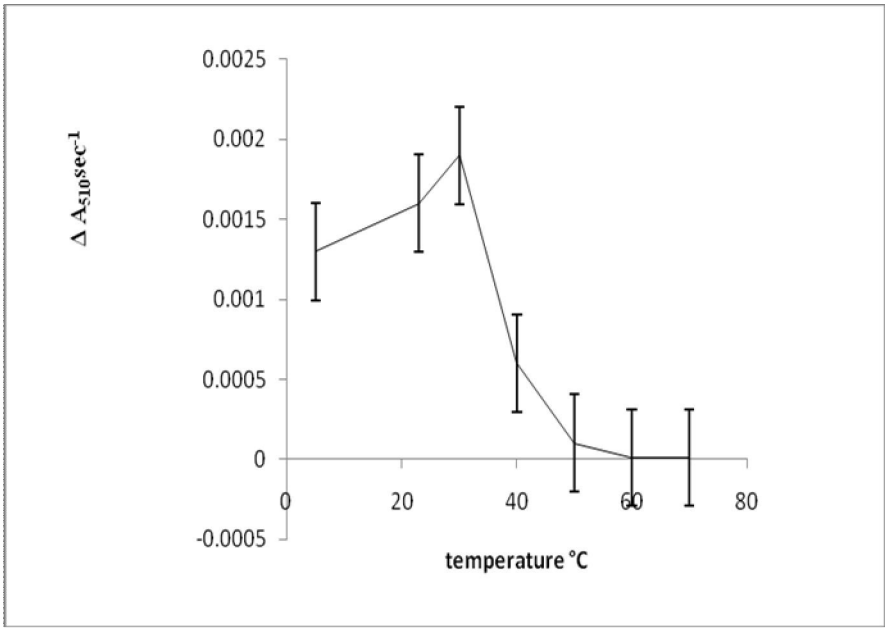

Figure 13: Effect of temperature on the rate of protocatechuic acid oxidation by crude onion POD extract. [PA]= 10 mM, [H_2O_2] =2 mM, pH= 4.

3.1.1.2 Effect of pH covariance

Next, the optimum temperature for protocatechuic acid oxidation reaction was fixed and the effect of pH covariance was studied. It is found that an increase in the pH value increased the reaction rate until pH4, whereas it became linear (same reaction rate) between 4 and 5. Then the reaction rate increased to reach its optimum at pH6. However, higher pH variations were found to decrease the reaction rate, which became very low between pH7 and 8 (**Figure 14**).

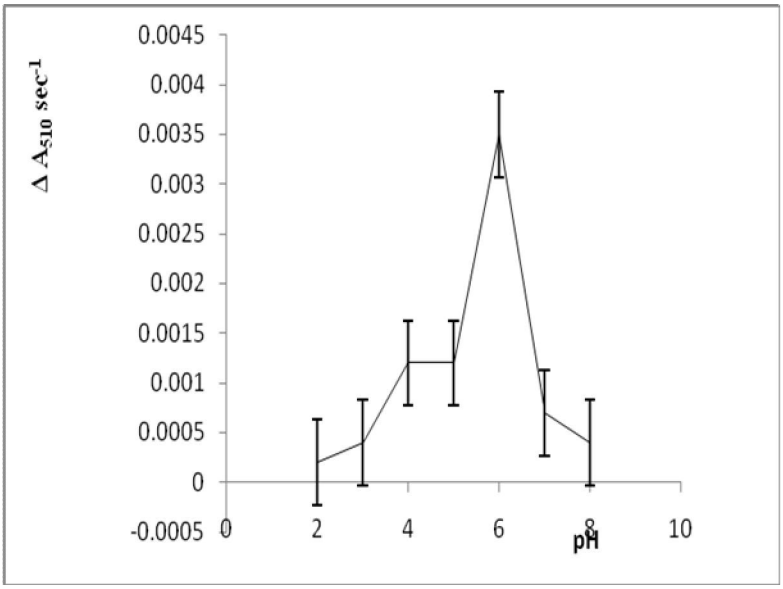

Figure 14: Effect of pH on the rate of protocatechuic acid oxidation by crude onion POD extract. [PA]=10 mM, [H_2O_2] = 2 mM, T= 30ºC and pH6.

3.1.1.3 Effect of H_2O_2 concentration covariance

Subsequently, the optimum temperature and the optimum pH values were fixed, and the effect of H_2O_2 concentration on the reaction rate was studied. A low increase in the concentration of H_2O_2 showed a high increase in the reaction rate of onion POD extract. The onion POD reaction rate on PA increased successively with the increase of H_2O_2 concentration to reach its maximum at 0,8mM (H_2O_2). Then the reaction rate decreased subtly after that with an increase in the concentration of H_2O_2 (**Figure 15**).

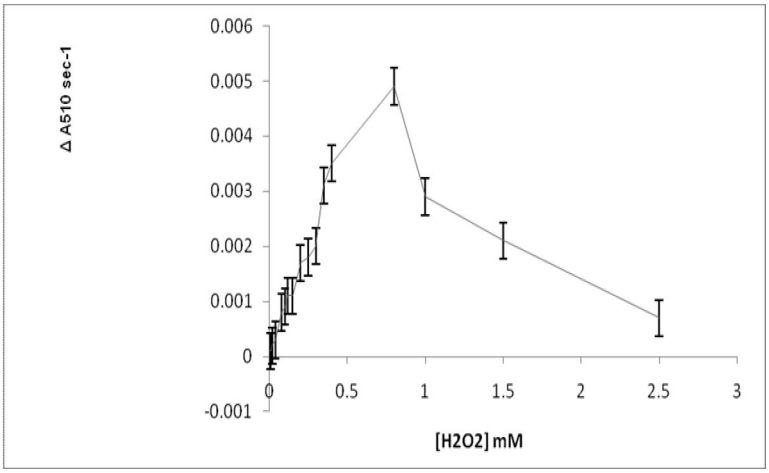

Figure 15: Effect of H_2O_2 concentration on the rate of oxidation by crude onion POD extract. $[H_2O_2]$= 0,8mM, pH6, T=30°C.

3.1.1.4 Effect of substrate concentration covariance

Examination of the effect of substrate concentration changes revealed high enzyme activity at concentration higher than 0,3mM. The change in enzyme reaction rate increase quickly from 0,3 to 0,8 mM. After that it continued to increase slowly with the increase on the substrate concentration to reach its optimum at 2mM. Then significant decline was shown when the enzymic reaction was carried out with higher substrate concentrations (**Figure 16**).

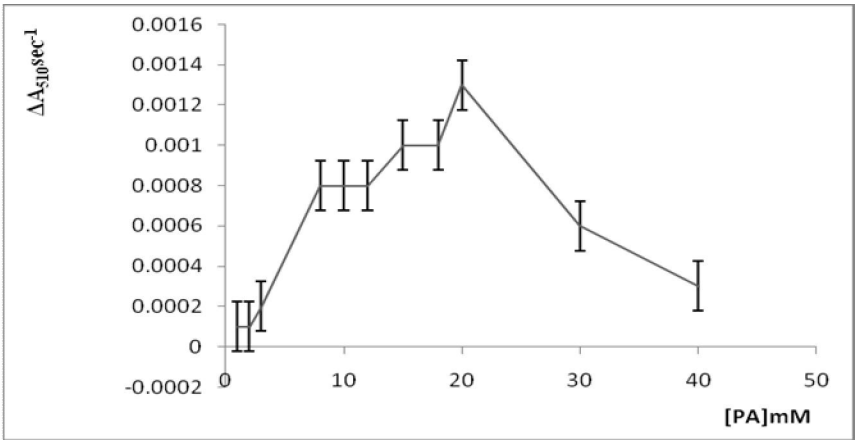

Figure 16: Effect of protocatechuic acid concentration on the rate of substrate oxidation by crude onion POD extract. $[H_2O_2]$=0,8mM, pH 6, T=30ºC.

3.1.1.5 Effect of enzyme dilution covariance

By implementing optimal conditions with regard to temperature, pH, H_2O_2 concentration and PA concentration, different dilutions of the enzyme homogenate were assayed (**Figure 17**). Increasing amounts of total protein in the reaction mixture provoked proportionally higher enzyme activities, suggesting that the rate of PA oxidation is directly proportional to the total enzyme concentration.

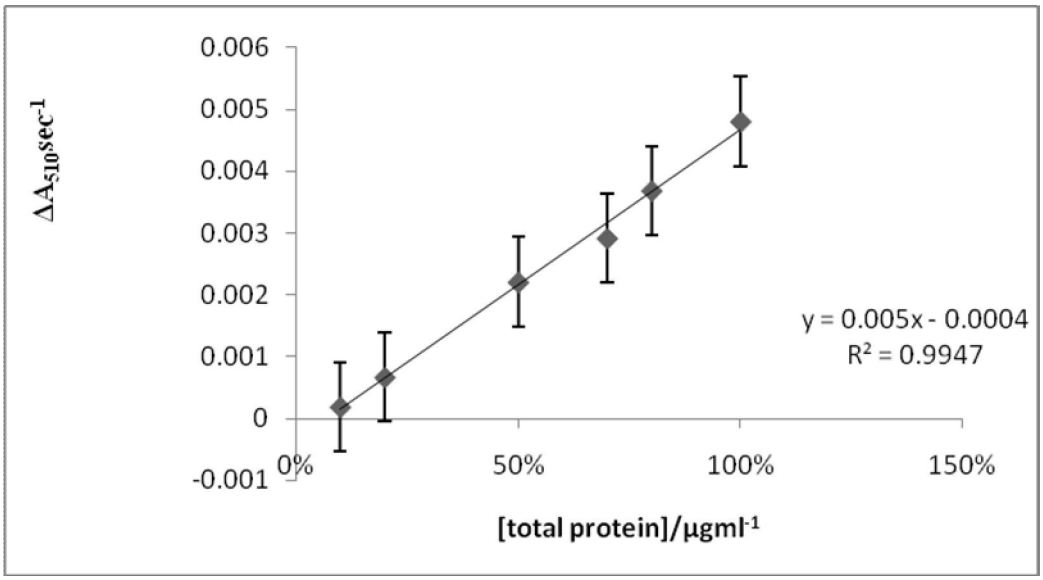

Figure 17: Effect of protein dilution on the rate of protocatechuic acid oxidation by crude onion POD extract. [H_2O_2]=0,8mM, pH 6, T=30ºC, [PA] =2 mM.

Peroxidises catalyze the oxidation of a wide variety of substrates, using H_2O_2 or other peroxides and lead to the formation of more complex structures such as the formation of dimers, oligomers and polymers (El Agha et *al*., 2008; 2009 and Osman et *al*., 2008) from both ferulic and cafeic acid, as well as quercetin. In our experiment the oxidation of protocatechuic acid by crude onion POD extract using the LC-DAD-MS method at 278 nm and 340 nm did not yield the formation of any important oxidation products, fragments or complexes (with any importance from a biological point of view).

3.1.2 Optimization of the pentahydroxy chalcone cyclization process using response surface methodology

The values of the independent process variables (X_1, X_2 and X_3) considered, as well as the measured and predicted values for the response (aureusidin peak area), are given analytically in **Table 4**.

Table 4: Measured and predicted aureusidin peak area values determined for individual design points

Design point	**Independent variables**			**Responses**	
				Peak area (aureusidin)	
	X_1	**X_2**	**X_3**	**Measured**	**Predicted**
1	-1	-1	-1	277.8	283.1
2	-1	-1	1	324.8	308.7
3	-1	1	-1	0	-26.6
4	-1	1	1	0	-15.5
5	1	-1	-1	136.6	150.3
6	1	-1	1	156.1	180.8
7	1	1	-1	0	14.3
8	1	1	1	37.5	30.3
9	-1	0	0	0	52.9
10	1	0	0	54.9	9.4
11	0	-1	0	292.5	265.0
12	0	1	0	0	34.9
13	0	0	-1	0	-6.7
14	0	0	1	0	14.1
15	0	0	0	49.3	34.6
16	0	0	0	.	34.6

The experimental values of the aureusidin peak area were determined by multiple regressions so as to fit the second-order polynomial equation shown in **Table 4**. The curve fitting coefficient for second-order polynomial equations was checked using the coefficients of determination (R^2 = 0.95). Both the coefficients and the *p* value for aureusidin peak area indicated a satisfactory agreement between the observed and predicted responses. The *p* value determined

(**Table 4**) implied that the equation found for aureusidin yield can adequately predict the experimental results, as the fit was statistically significant ($p < 0.02$).

The coefficients for the incubation temperature and pH range were negative, indicating that increasing the incubation temperature and pH range are inversely proportional to the aureusidin formation yielding a weak amount of product cyclization, thus suggesting that aureusidin yield is favoured at low temperature (room temperature) and low pH (acidic pH). By contrast, the incubation time coefficients were positive, suggesting that the aureusidin formation is more favourable for longer incubation time.

Table 5: Polynomial equation and statistical parameters calculated after implementation of a 23 full-factorial design

Response variables	**2nd order polynomial equation**	**R^2**	***p***
Peak area (aureusidin yield)	$34.54-21.75X1-115.03X_2+10.4X_3+43.43X_1X_2+1.25X_2X_3-3.62X_1X_3-30.41X_1^2+115.39X_2^2-30.86X_3^2$	0.95	0.0083

These trends were recorded in three-dimensional response surface curves, using the polynomial equations. The plot shown in **Figure18** illustrates the combined effect of incubation time and pH on the aureusidin yield. It is clearly shown that low pH along with long incubation time increase the peak area of aureusidin.

3.1.2.1 Effect of time and pH covariance on pentahydroxy chalcone cyclization

pH range was shown to exhibit a profound effect on pentahydroxy chalcone cyclization, as shown in **Figure 18**. The highest amount was recorded at low pH values along with low temperature, whereas time did not have a strong effect on the reaction yield.

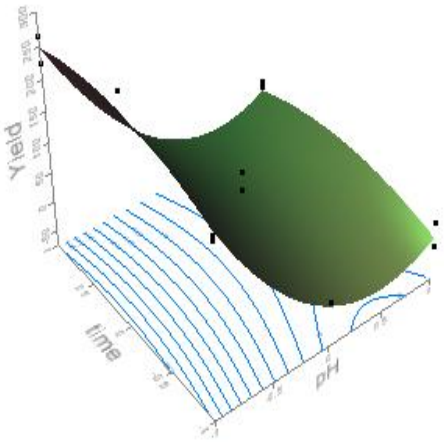

Figure 18: Response surface plot showing the effect of pentahydroxy chalcone cyclization time and pH covariance on the total aureusidin yield.

3.1.2.2 Effect of time and temperature covariance on pentahydroxy chalcone cyclization

Likewise, time appeared to promote pentahydroxy chalcone cyclization, as recorded in **Figure 19**. Under optimal conditions (temperature 20°C, pH5 and 5h incubation time) the highest aureusidin peak area was theoretically calculated to be 308.65±43.802, whereas at 3h and 1h incubation time the amount decreased by approximately 10% and 20% respectively.

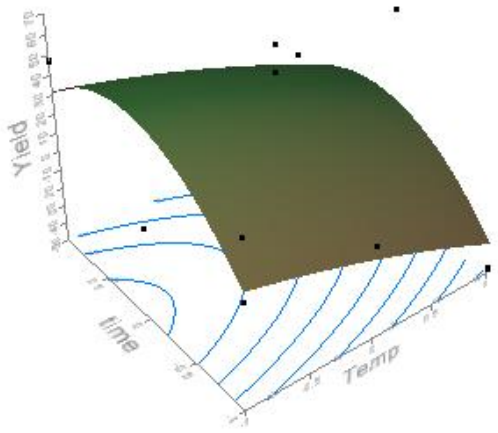

Figure 19: Response surface plot showing the effect of pentahydroxy chalcone cyclization reaction time and temperature covariance on the total aureusidin yield.

3.1.2.3 Effect of temperature and pH covariance on pentahydroxy chalcone cyclization

At the same time as recorded in **Figure 20** the temperature effect on aureusidin yield showed that when temperature is increased between 20°C and 30°C, it has negligible effect on the reaction yield, whereas from 30°C to 40°C it shows a more than 50% decrease.

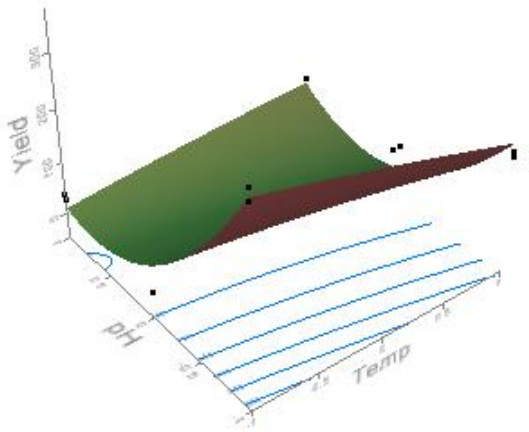

Figure 20: Response surface showing the effect of pH and temperature covariance on the aureusidin yield.

3.1.2.4 Linear regression analysis between the aureusidin predicted and measured yield

Simple linear regression analyses indicated that the aureusidin yield obtained is linked in a statistically significant manner **Figure 21**. All the results obtained fit the confidence interval except one point with no yield while the correlation with actual and predicted yield was strong (R^2= 0.95 with p = 00.83 and RSME = 43.802). The actual and predicted yield were very low when the analysis conditions (pH, temperature and time) do not fit the optimum (no aureusidin formation or low peak area corresponding to the six points with no yield and the three points around 50). An acceptable peak area (the two points around 150) was recorded when the conditions fit only one parameter (optimum pH without time and temperature). When all the three parameter are around the optimum, a considerable yield (peak area) was recorded with an optimum obtained at temperature 20°C, pH 5 and 5h incubation time as shown in **Figure 21**.

From the figure of simple linear regression analyses we can conclude that the cyclization yield is considerably influenced by the pH, then by time and temperature of the reaction medium, suggesting more optimization reaction using pH combined with other parameters such as the concentration of the substrate and the concentration of the activator H_20_2.

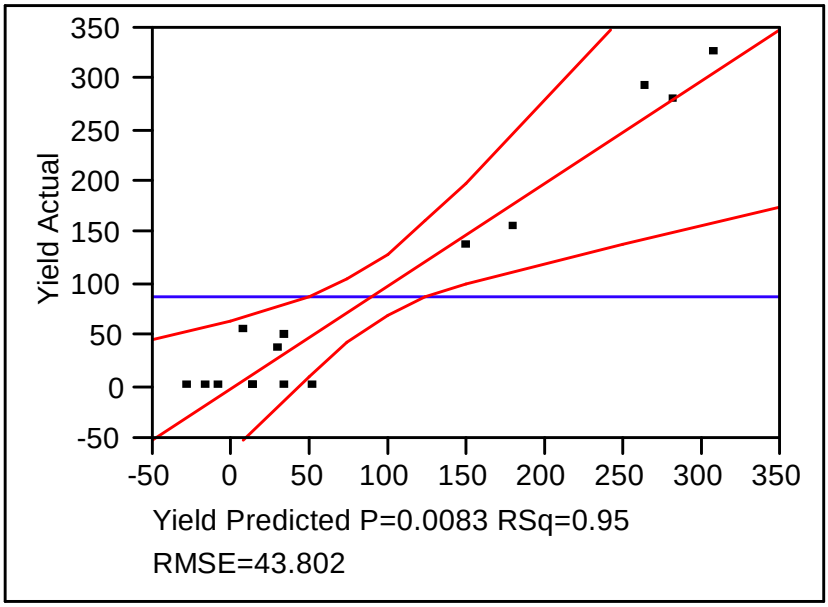

Figure 21: Linear regression analysis between the predicted aureusidin and measured yield for pentahydroxy chalcone as a substrate with onion POD extract.

The novel outcome of this work is that a cheap, crude POD enzyme extract from agrifood waste (onion case) can be valorised for the "green" preparation of bioactive aurones from chalcones, which are easily synthesised through the Claisen-Schmidt condensation (data under publication; Sheng Cheng et *al*., 2000 and Dickson et *al.*, 2006) or from natural ones.

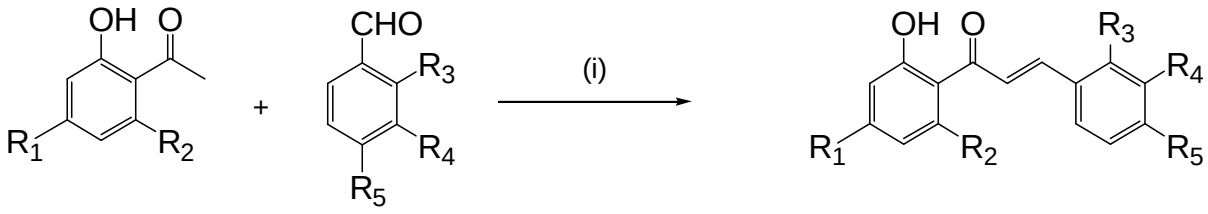

i: 20% aqueous KOH, MeOH, r.t., 24-36h

Figure 22: Chalcone synthesis by the Claisen Scmidt condensation

In this view it is important to underline that a crude peroxidase from onion, not a chalcone specific, behaves in the same way as aureusidin synthase. To demonstrate the possibility of preparative applications of the extract, a scale up reaction was performed as described in page 26.

3.1.3 Onion POD scale up reaction using Pentahydroxychalcone as a substrate

3.1.3.1 LC-DAD-MS analysis of pentahydroxy chalcone with onion POD

The starting material was 15mg pentahydroxy chalcone and the incubation time 3 hours. The reaction was monitored by LC-DAD-MS at 370nm (chalcones), 400nm (aurones) and 278nm (**Figure 23**); the MS conditions were as follows: 4kV and 350 °C (ESI probe) at 12 and 40 eV (collision induced dissociation energies) with a scanning rate of 0.8 scans per second in the range of 121-787 amu. The starting material disappeared, and 2 major peaks appeared together with a minor one. According to the UV-Vis spectra the peaks at 7.75 and 8.28 min are indicative of aurone scaffold (**Figure 24**), whereas the minor product at 7.96 min must be the flavanone side product which is usually formed from chalcones, as discussed below (pages 43-50). After workup of the reaction mixture, the crude residue was purified on preparative reverse phase TLC (RP18; 10X20cm; thickness of 0,25mm; Merck) using 60:40/ methanol w/ 2,5% acetic acid : water for the first elution. The plate was dried and a second elution with 75:25 / methanol w/ 2,5% acetic acid : water followed. The separation was monitored under UV. The bands of the eluted products were scraped off and extracted with methanol. Approximately 8mg were isolated for the expected aurone (aureusidin) at 7.75min (also identified against synthesised standard by HPLC, see page 40) and

5mg for the peak at 8.28 min. The structure of the second product was tentatively assigned to that of a dimer as discussed and argumented in pp 47 – 53.

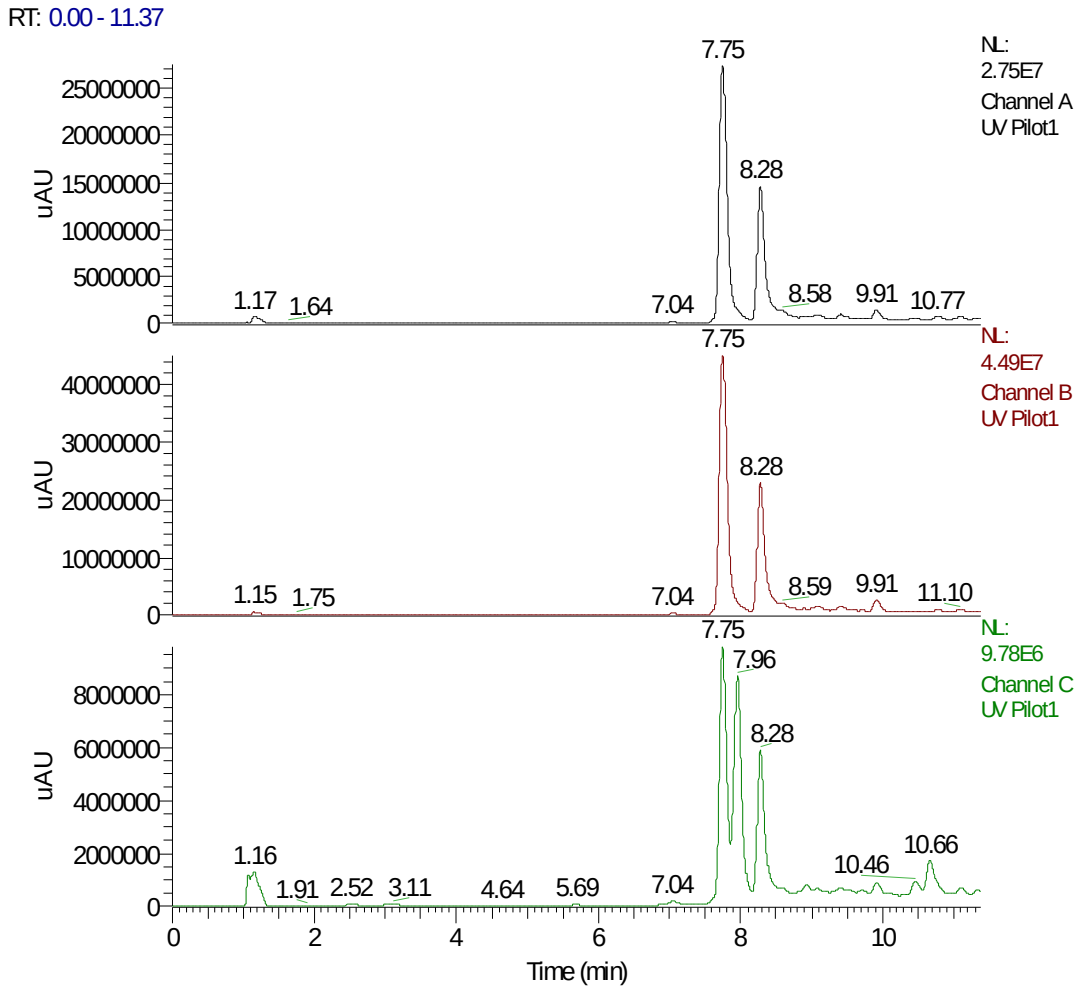

Figure 23: HPLC chromatogram of pentahydroxy chalcone with onion POD. Final pentahydroxy chalcone and H_2O_2 concentration in the reaction medium are 2 mM; [H_2O_2] = 3 mM; pH = 5; T=20 ^{0}C. Incubation time = 3 hours.

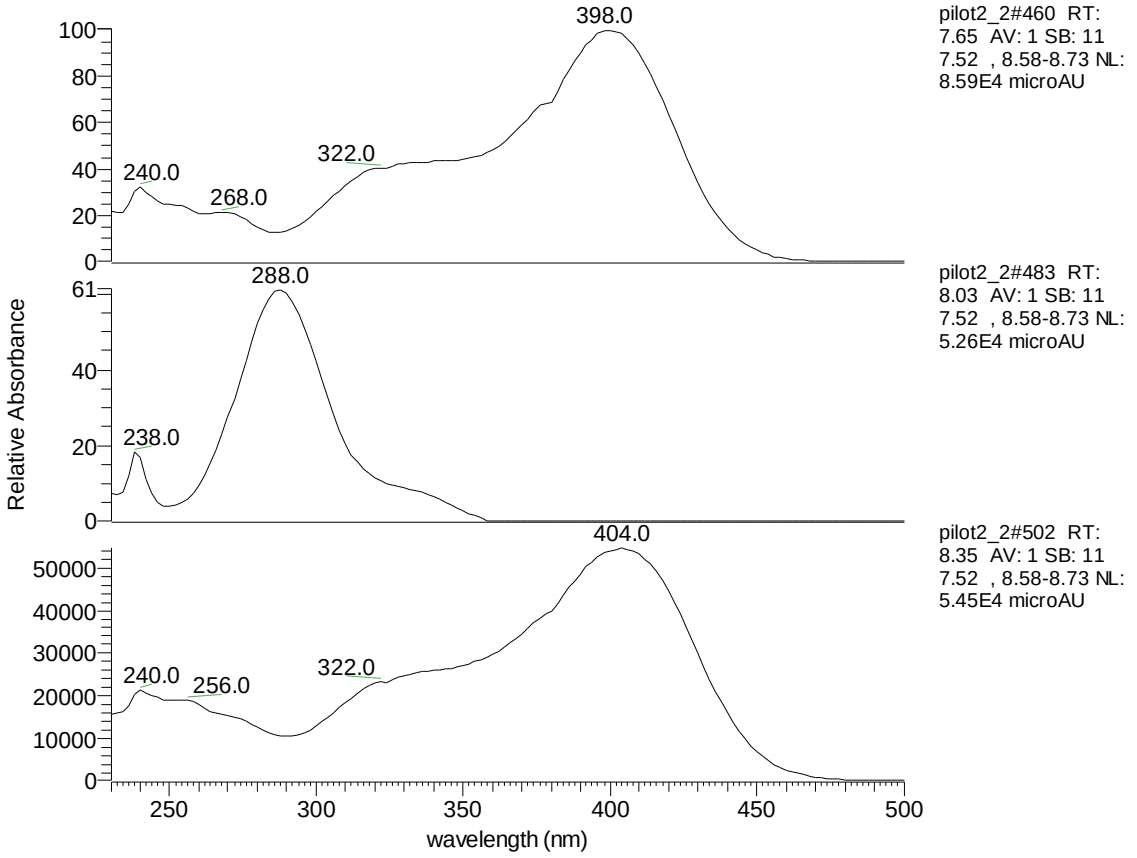

Figure 24: UV-Vis spectra of aureusidin, side flavanone and aureusidin dimer, respectively.

The mass spectrum of aureusidin is shown in **Figure 25** in full agreement with that of the synthesized standard. M+1=287 (214 is an artefact fragment of background noise)

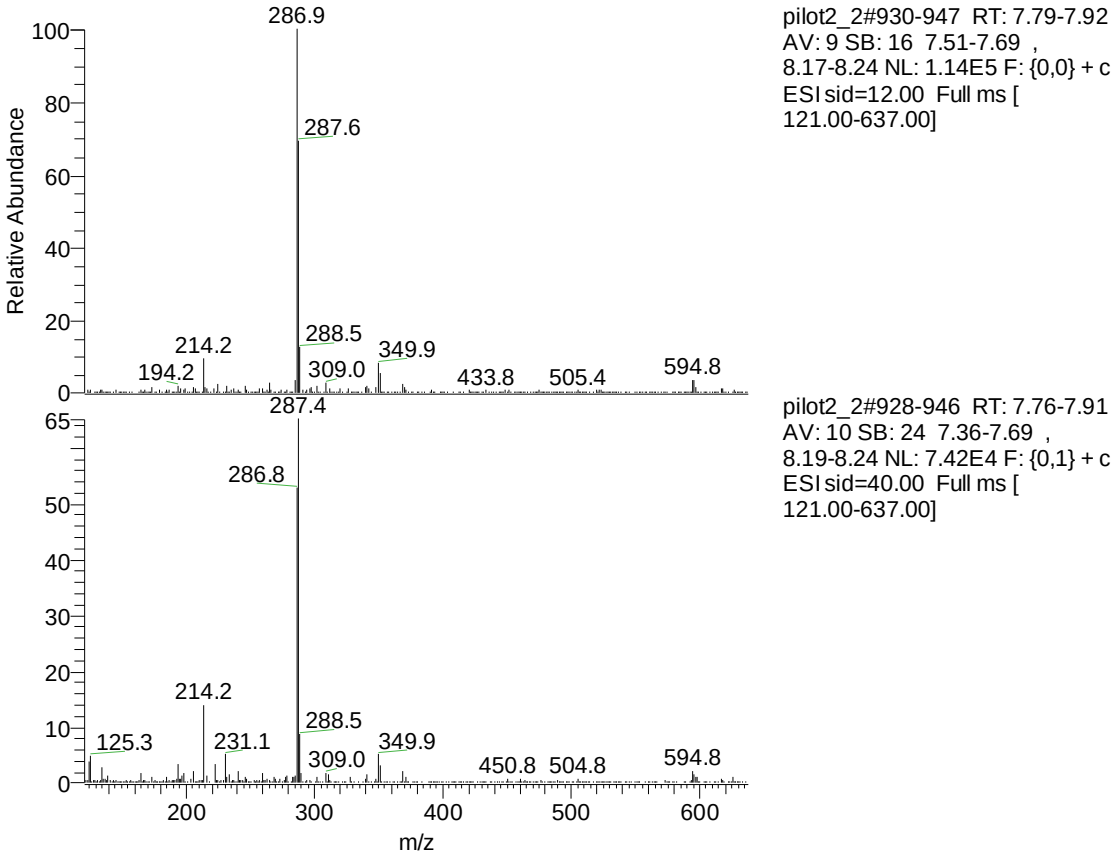

Figure 25: Mass spectrum of aureusidin from the onion POD reaction

.

3.1.3.2 Proposed structure of aureusidin and side reaction fragments issued from pentahydroxy chalcone with onion POD

The structure of the product is further propped up by ^{1}H NMR spectroscopy (300MHz; CD_3OD) as shown below (**Figure 26**). The spectrum was recorded on a Varian Gemini 2000 300 MHz spectrometer at the Technical University of Athens, Greece.

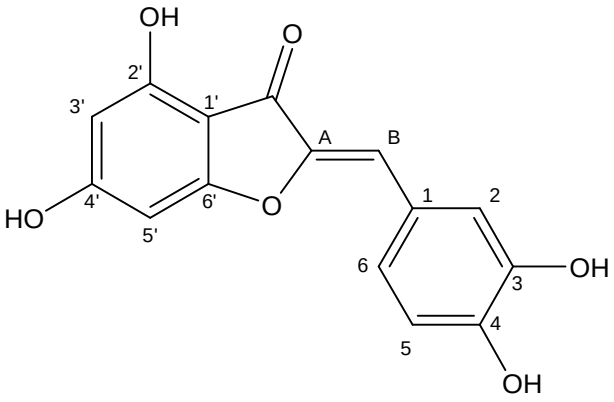

Figure 26: Aureusidin structure

Table 6: Aureusidin ^{1}H NMR data

7,472 ppm	d, H-2	$J_{2,6}$ =1,83Hz
7,179	dd, H-6	$J_{6,5}$=8,43Hz; $J_{6,2}$=1,83Hz
7,822	d, H-5	$J_{5,6}$ =8,43Hz
6,568	s, H_B	
6,172	bs, H-3’	
5,998	bs, H-5’	

Compound at 7,96 min: The absorption at 288nm and the form of the UV-Vis spectrum (Marby et *al.*, 1970) betray formation of a flavanone (5,7,3’,4’ tetrahydroxy flavanone) explained by the mechanism given in **Figure 27**. Chalcones may find themselves in equilibrium

with the closed flavanone ring (Gonzalez et *al.*, 2002). On the other hand the proposed structure is further supported by the MS spectrum of **Figure 28**, where M+1= 289, as expected. The identification of fragments 163 and 153 and 233 is given in **Figures 29**, **30** and **31**. Fragments 153 and 163 are explained by proton transfer mechanisms, whereas 233 is based on positive radical formation (Schâfer et *al*., 2007).

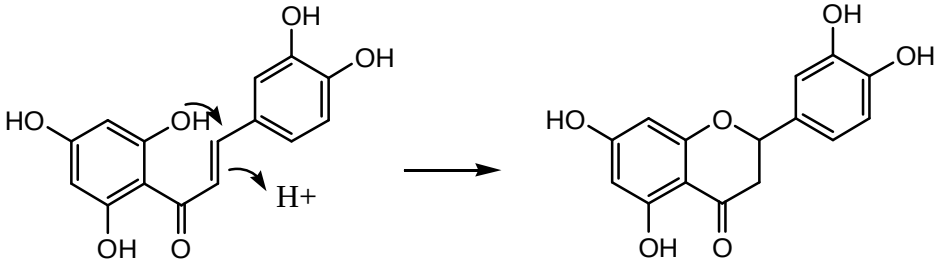

Molecular Weight: 288,25 Molecular Weight: 288,25

Figure 27: Cyclisation of a chalcone into a flavanone

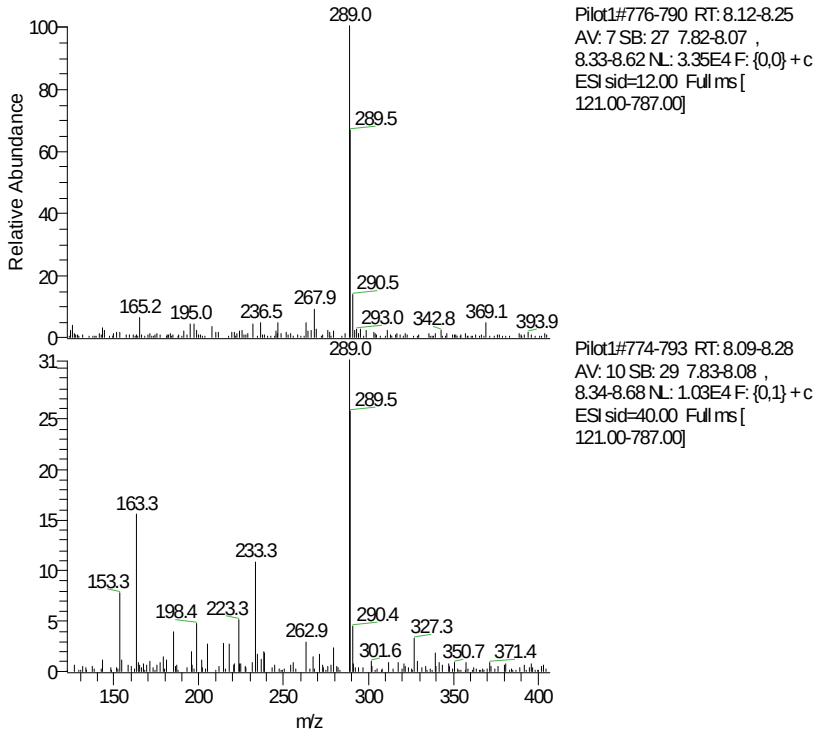

Figure 28: Mass spectrum of 5,7,3',4' tetrahydroxy flavanone formed through side reaction.

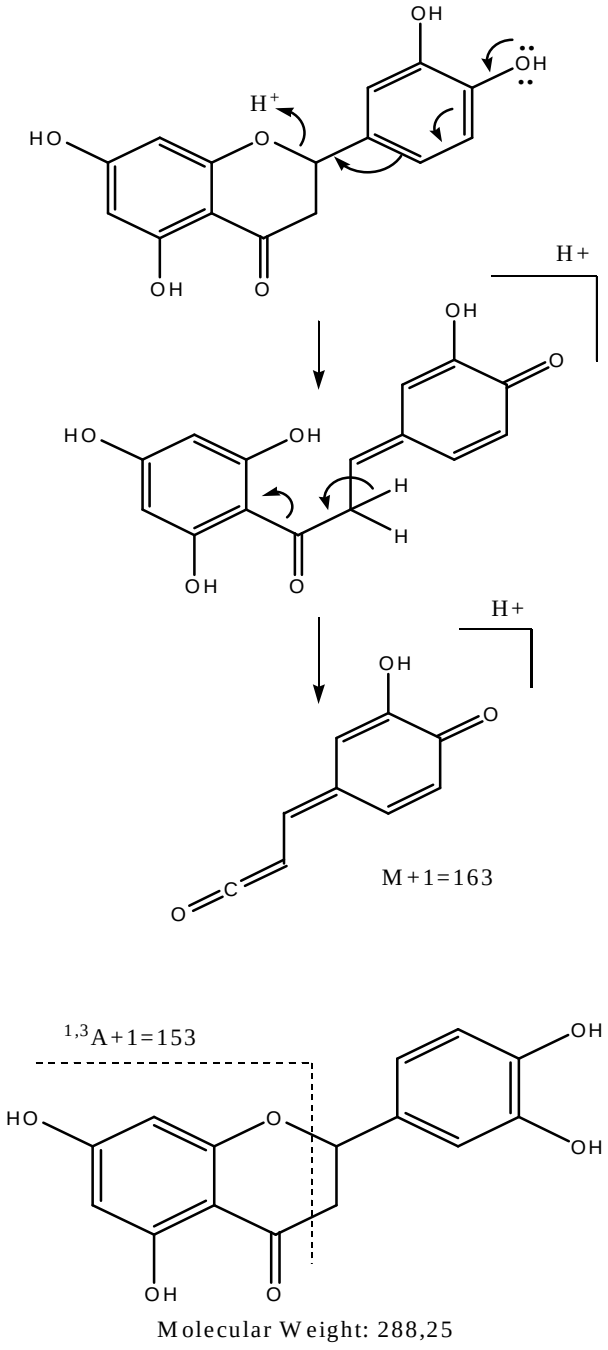

Figure 29: 5,7,3',4' tetrahydroxy flavanone proposed fragmentation leading to fragments 153 and 163. 1,3A is a symbol of mass fragmentation nomenclature according to Cuyckens et al. (2000).

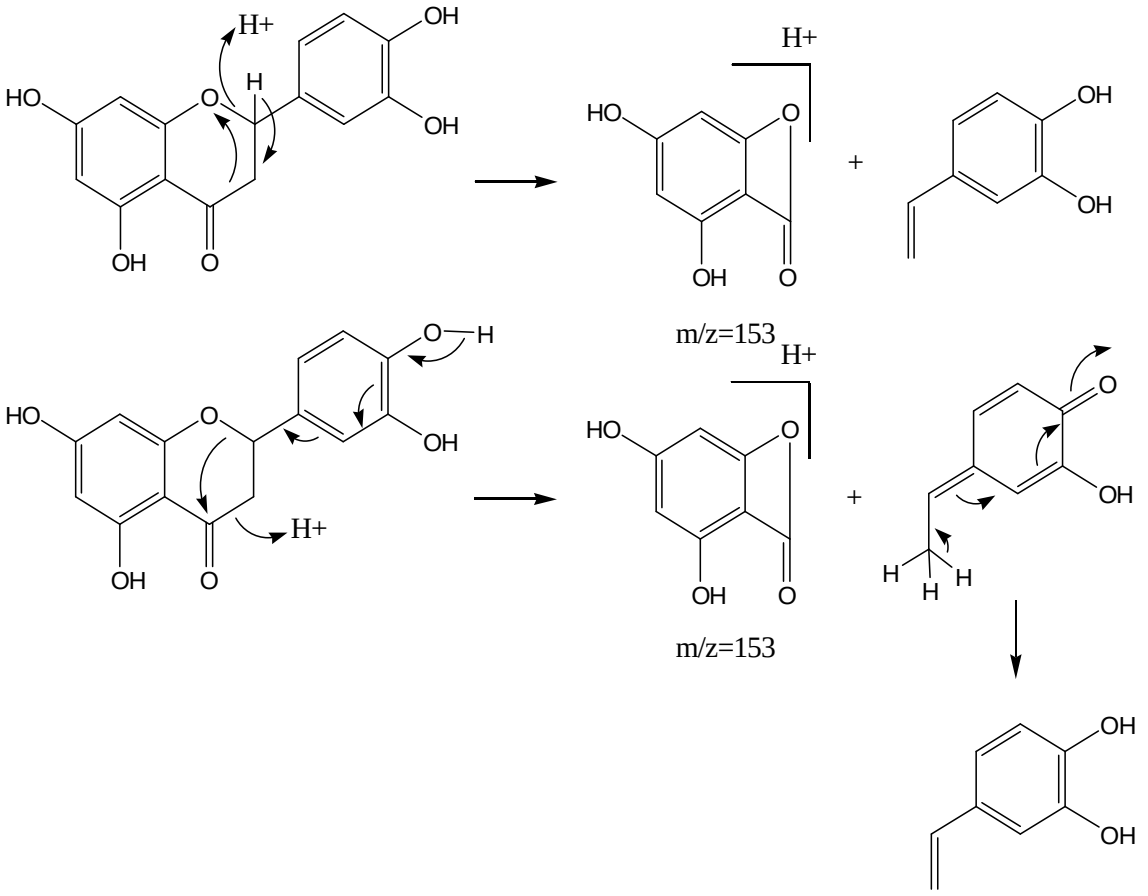

Figure 30: Proposed mechanism for fragment 153

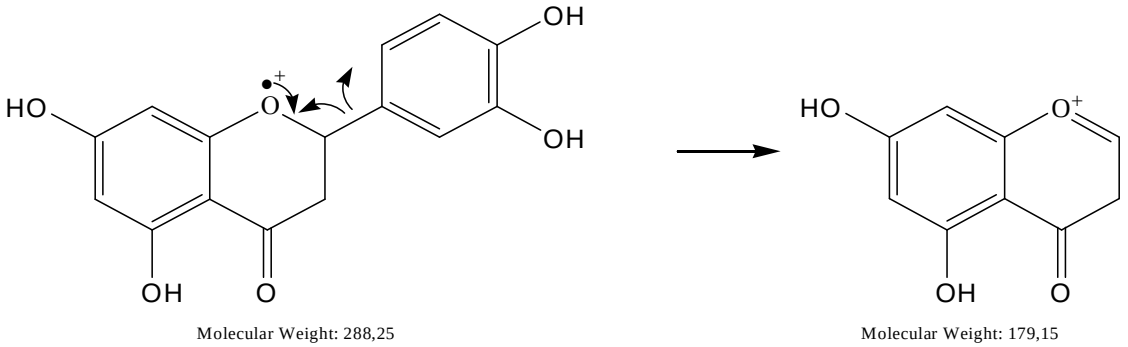

Figure 31: Fragment 233 from the flavanone explained through radical formation under ESI+ conditions

3.1.3.3 Proposed structure of aureusidin dimer issued from pentahydroxy chalcone with onion POD

The compound that elutes at 8,28 min has the typical UV-Vis spectrum of an aurone (Marby et *al.*, 1970) with a λmax at 404 nm and a presumable M+1 molecular ion of 571amu. Apparently, 593 = $M+Na^+$. A molecular ion of 571 meaning that the MW of the compound is 570 may be tentatively explained by a dimer formation (2x286 -2H = 570) from the areusidin structure in the reaction mixture. On the other hand, the fact that the UV-Vis spectrum and maximum are almost the same as for aureusidin leads to the suggestion that the bond between the two molecules is not formed in a way that a strong hypsochromic effect would be produced. Thus, position 4 must remain free. Also, the fact that a single LC peak corresponds to this compound suggests a bond creation that would not lead to diastereomer formation. In this sense, should a bond be formed between benzene rings, it would lead to various products, given that from previous experience when benzene-benzene bond formation occurs, under onion POD reaction, it is not regiospecific as found in works by El Agha et *al.(* 2008; 2009) and Osman et *al.*, (2008). Three main fragments are recorded in the spectra (**Figure 32**): 405, 303 and 289.

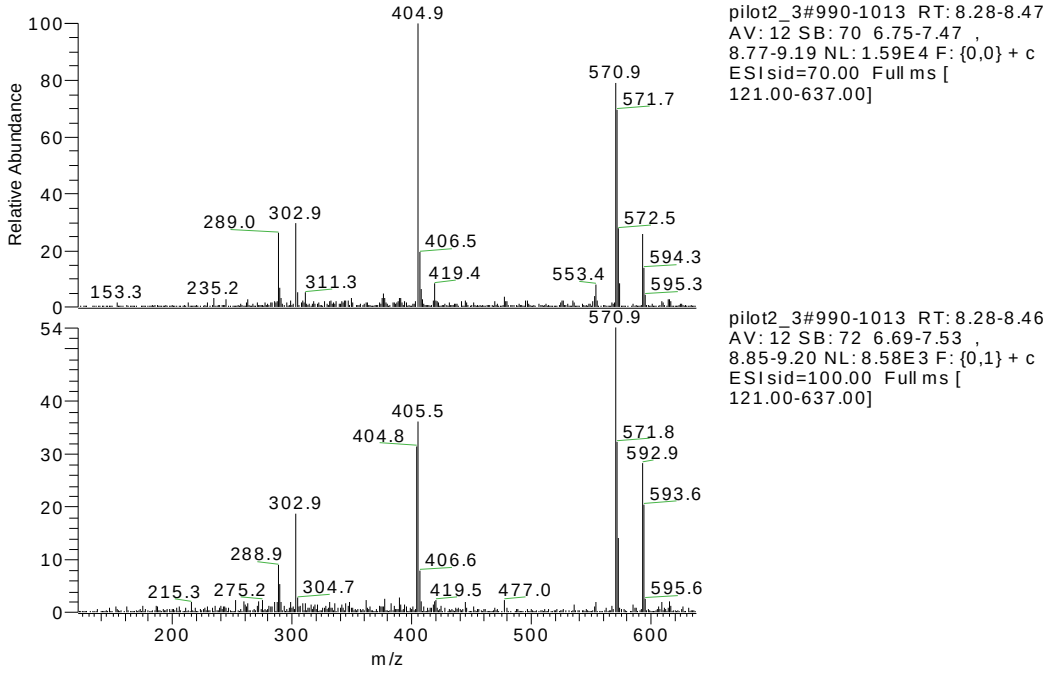

Figure 32: ESI spectra of the aureusidin dimer.

Following the hints and considerations displayed above, the structural assumption of a C-C bond formation between the two tertiary sp^2 carbons of the AB double bond (**Figure 32**) is the only one which provides mechanistic explanation for these three fragments (see **Figures 33, 34 and 35**). Fragments 405 and 303 are explained by proton transfer, where a maximum π electron delocalization stabilizes intermediate structures. Fragment 289 (**Figure 34**) is explained via a mechanism of radical homolytic fission of the bond between the olefinic carbons and neutral loss of carbon monoxide.

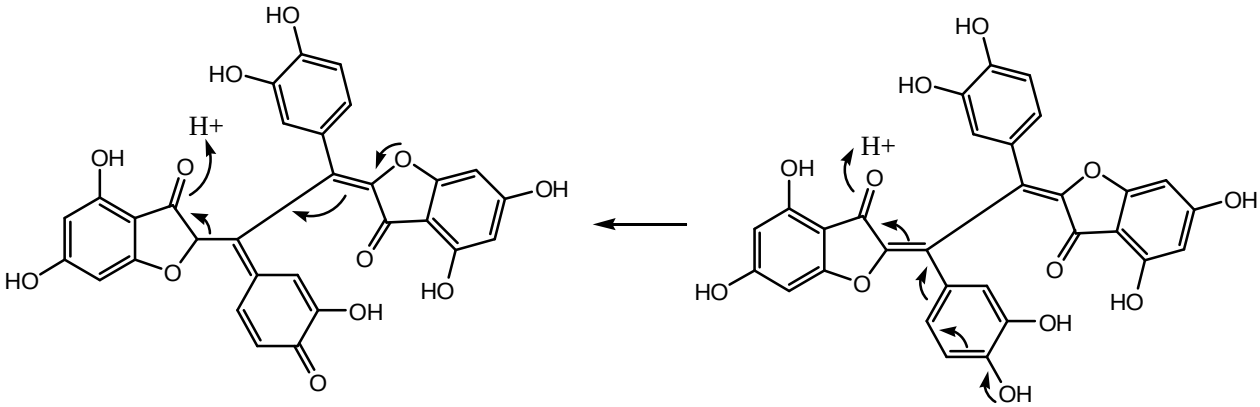

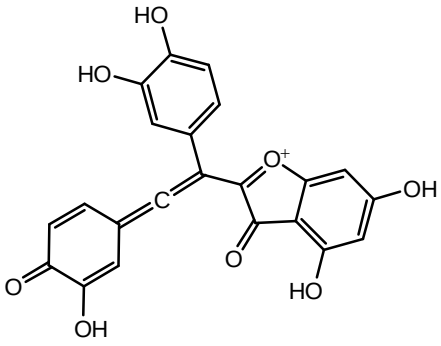

Figure 33: Mechanism for fragment 405.

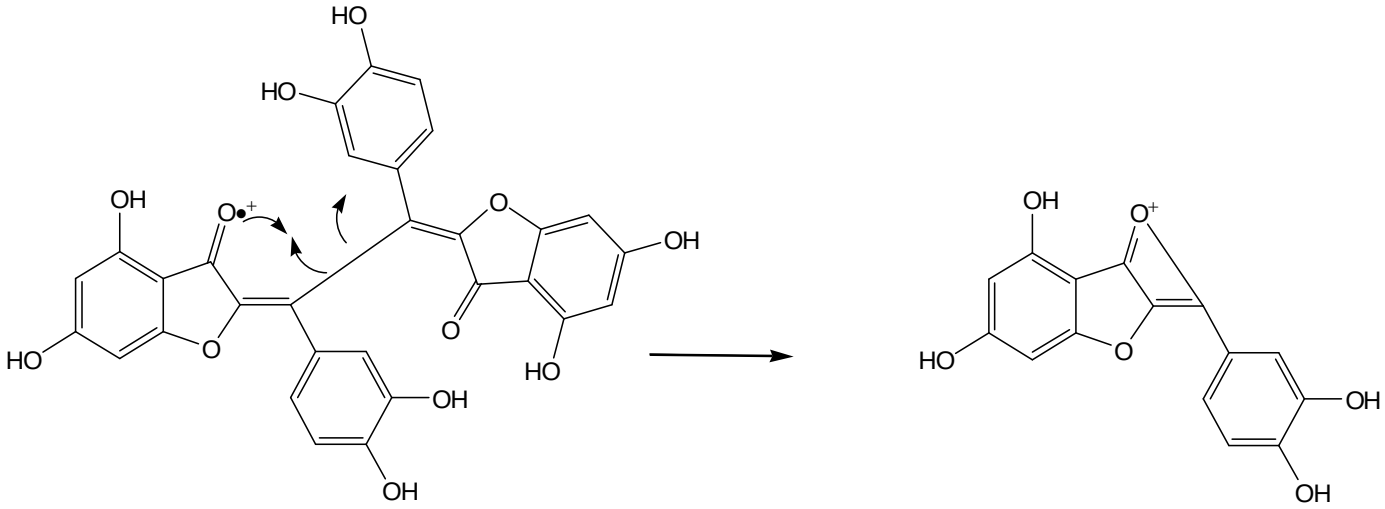

Molecular Weight: 285,23

Figure 34: Mechanism for fragment 289. m/z 289= 285-CO+MeOH=285-28+32

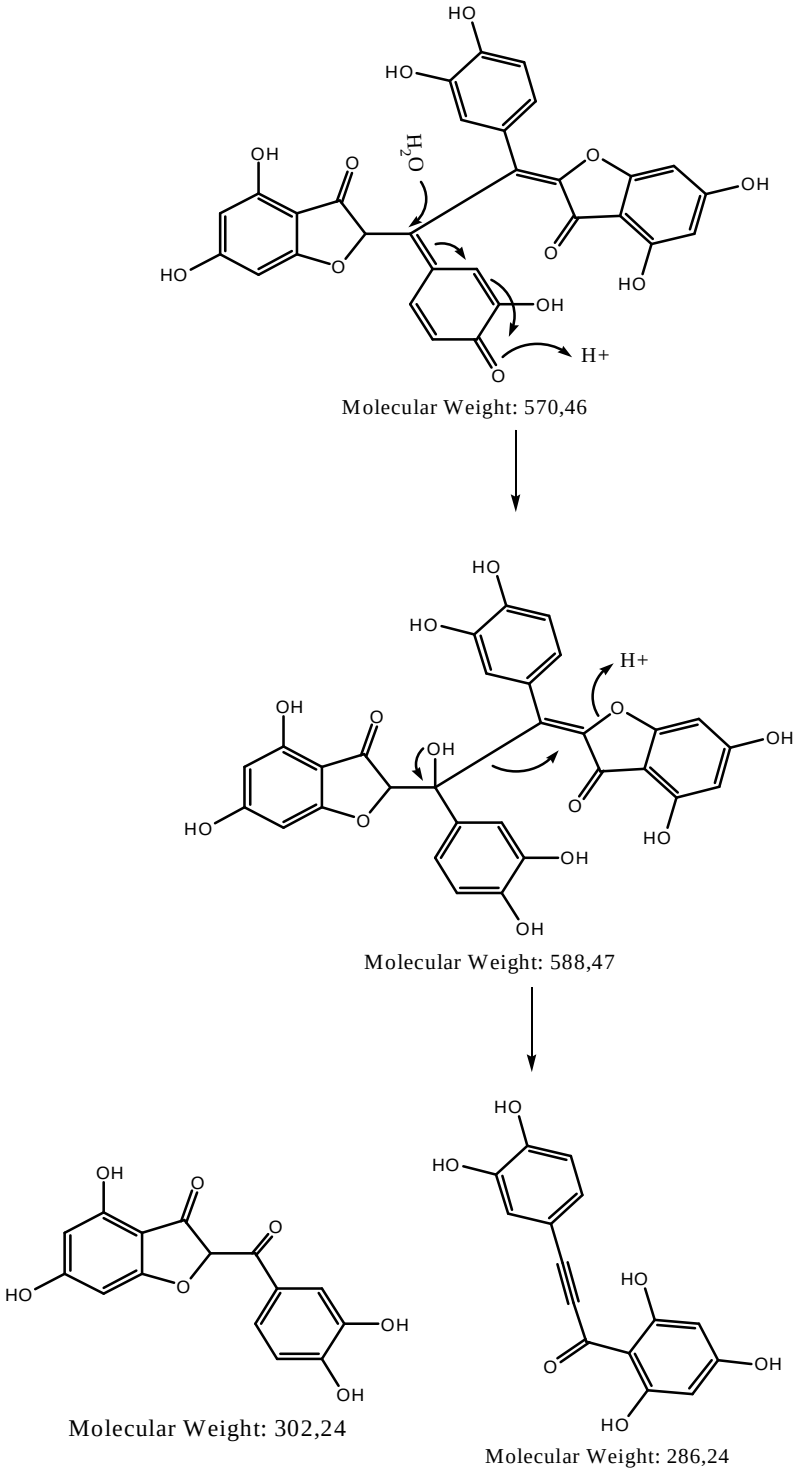

Figure 35: Mechanism for fragment 588, 302 and 286. m/z 303=302+1; m/z 286+1 is not observed

3.1.3.4 Structure and NMR data of aureusidin dimer issued from pentahydroxy chalcone with onion POD

The proposed structure is further supported by the NMR spectrum in deuterated methanol (300MHz, as for aureusidin).

Table 7: NMR data of aureusidin dimer in deuterated methanol (300MHz, as for aureusidin)

7,499 ppm	d, H-2; d, H-2''	$J_{2,6}$ =1,83Hz= $J_{2'',6''}$
7,169	dd, H-6; dd, H-6''	$J_{6,5}$=8,00Hz= $J_{6'',5''}$; $J_{6,2}$=1,83Hz= $J_{6'',2''}$
6,815	d; H-5; d, H-5''	$J_{5,6}$ =8,00Hz=$J_{5'',6''}$
6,161	d, H-5'; d, H-5'''	$J_{5',3'}$ =1,53Hz= $J_{5''',3'''}$
6,057	d, H-3'; d, H-3'''	$J_{3',5'}$ =1,53Hz= $J_{3''',5'''}$

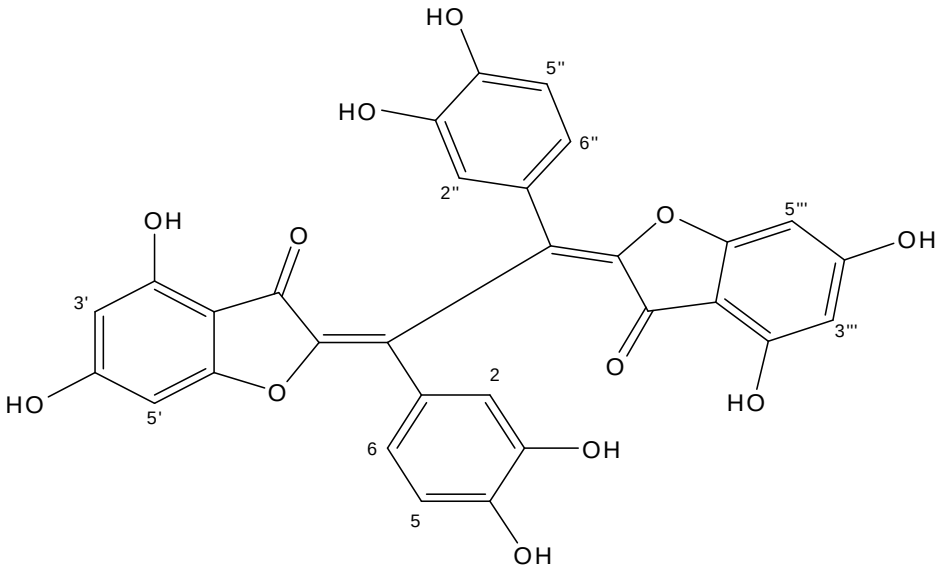

Figure 36: Aureusidin-dimer (Structure and 1H NMR data)

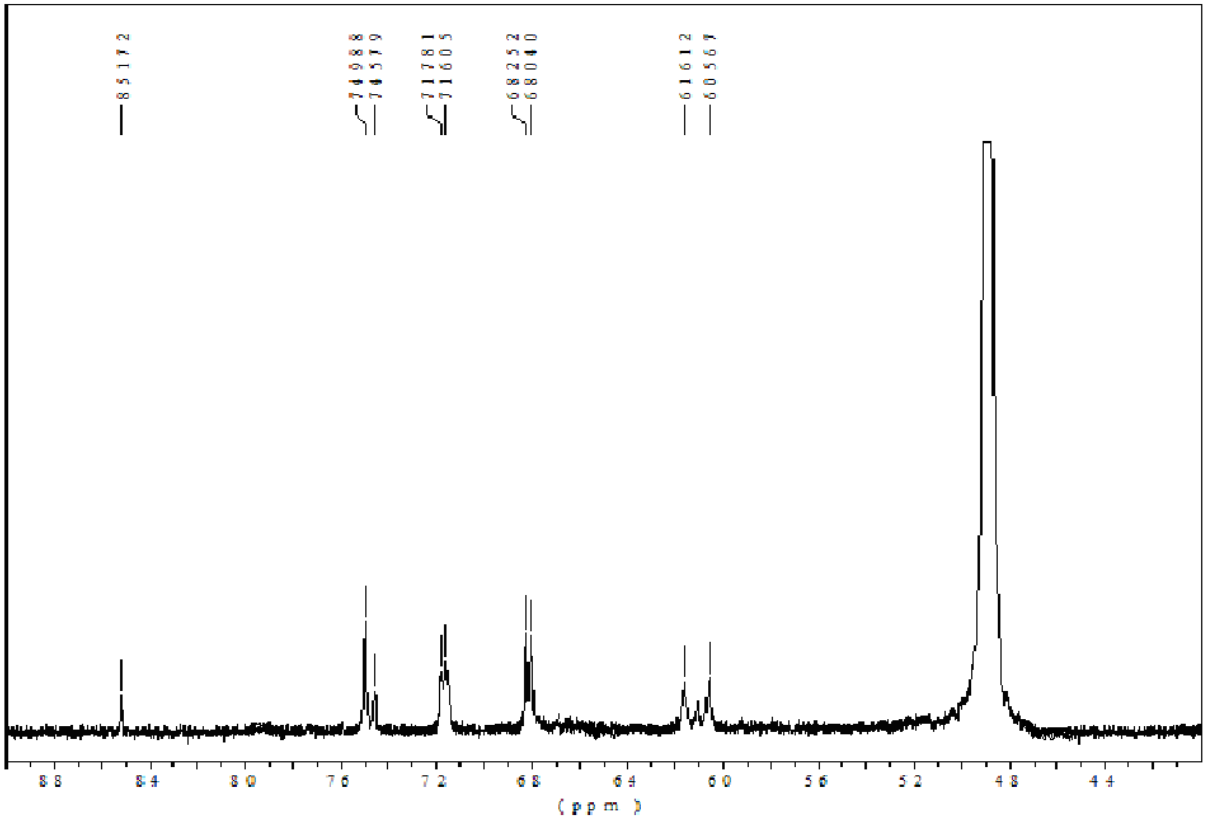

Figure 37: H1-NMR of aureusidin-dimer

At this point it is of importance to mention that a very similar structure to our compound in question has been identified by Westenburg et *al*., (2000) and is shown below in **Figure 38**.

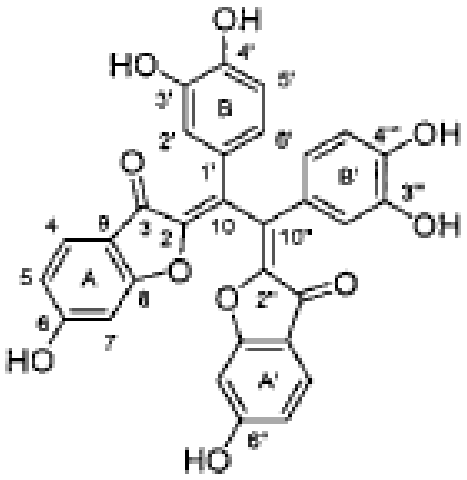

Figure 38: Structure of aureusidin dimer or disulfuretin {2,2'-[1,2-bis(3,4-dihydroxyphenyl)-1,2-ethanedylidene]-bis[6-hydroxy-3(2H)-benzofuranone}.

Last but not least, why the dimer was not observed in the low scale reaction? Given that the scale up took place by full respect of analogies (concentrations and volumes) and conditions to the exception of DMF concentration, the apparent tentative explanation seems to be born on it. In other words increase of the DMF concentration as we move from high scale to low suppresses dimer formation.

3.1.4 Onion POD scale up reaction using 4,2'-dihydroxychalcone as substrate

3.1.4.1 LC-DAD-MS analysis of dihydroxy chalcone with onion POD

As in page 26, an oxidative cyclisation of 4,2'-dihydroxychalcone (**Figure 39**) was attempted using onion POD extract. Note that the structural difference with the starting material on page 26 is that 4,2'-dihydroxychalcone does not have an ortho hydroxyl group. According to Strack and Schliemann (2001) a catechol system must be present on the B ring for the oxidative cyclisation to occur. We undertook this reaction in view of observing the activity of our onion POD extract on the non-catechol system chalcone. The starting material appears at RT: 12.9 min following the same elution conditions as for p. 26 (**Figure 40 and 41**). The peak at 15.3 min is

an impurity. The dihydroxychalcone was provided by Dr. Detsi (Laboratory of Organic Chemistry, School of Chemical Engineering, National Technical University of Athens, Greece).

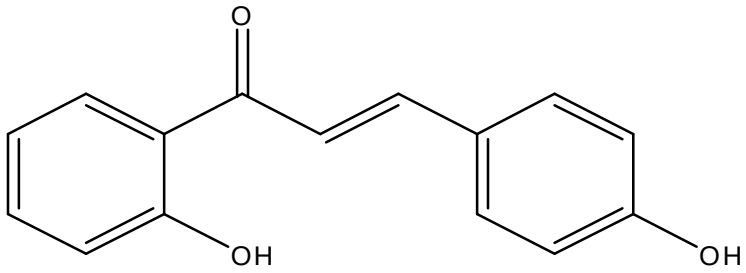

Molecular Weight: 240,25

Figure 39: Structure of 4, 2'-dihydroxychalcone

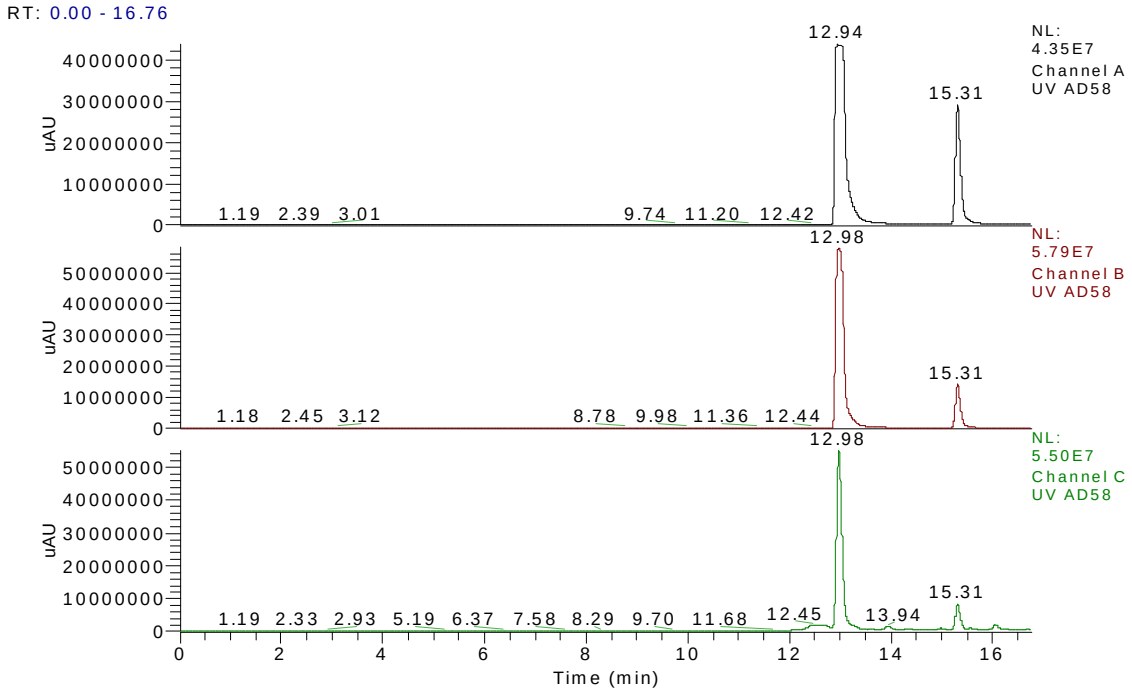

Figure 40: HPLC chromatogram at 370, 400, 278 nm

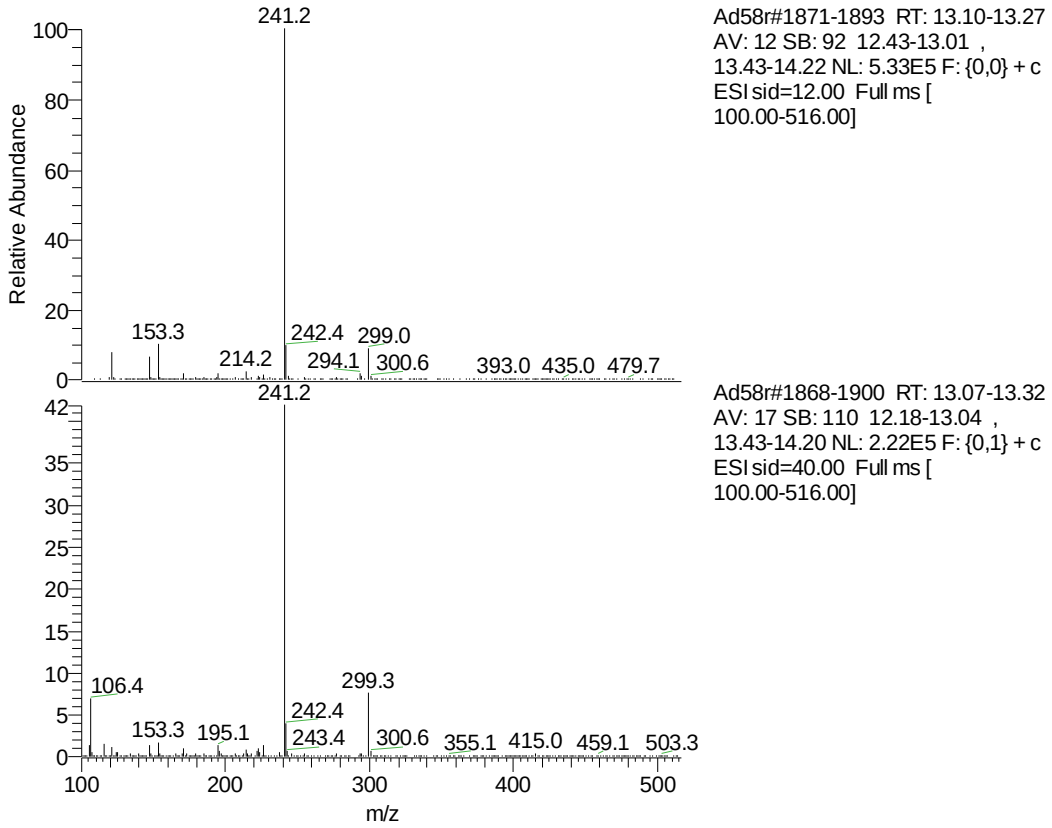

Figure 41: UV-Vis and MS spectra of 4,2'-dihydroxychalcone

3.1.4.2 Proposed structure of aureusidin, chalcone dimer and side product from dihydroxy chalcone with onion POD

After 1.5 h of reaction the starting material practically disappears (**Figure42**) and the corresponding aurone is tentatively intercepted as a minor product (**Figure43**). The UV-Vis and MS data support this assumption.

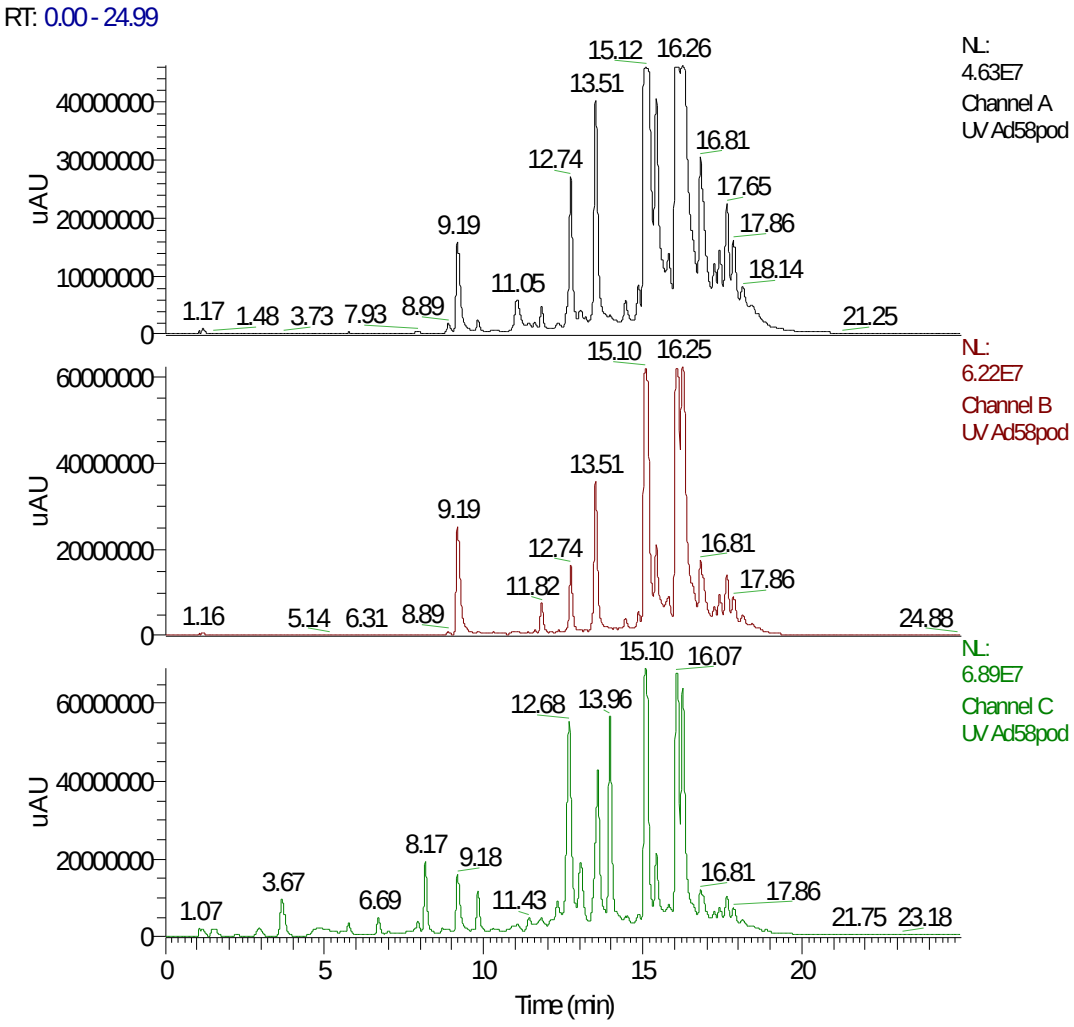

Figure 42: Reaction of 4, 2'-dihydroxychalcone with the onion POD extract

.

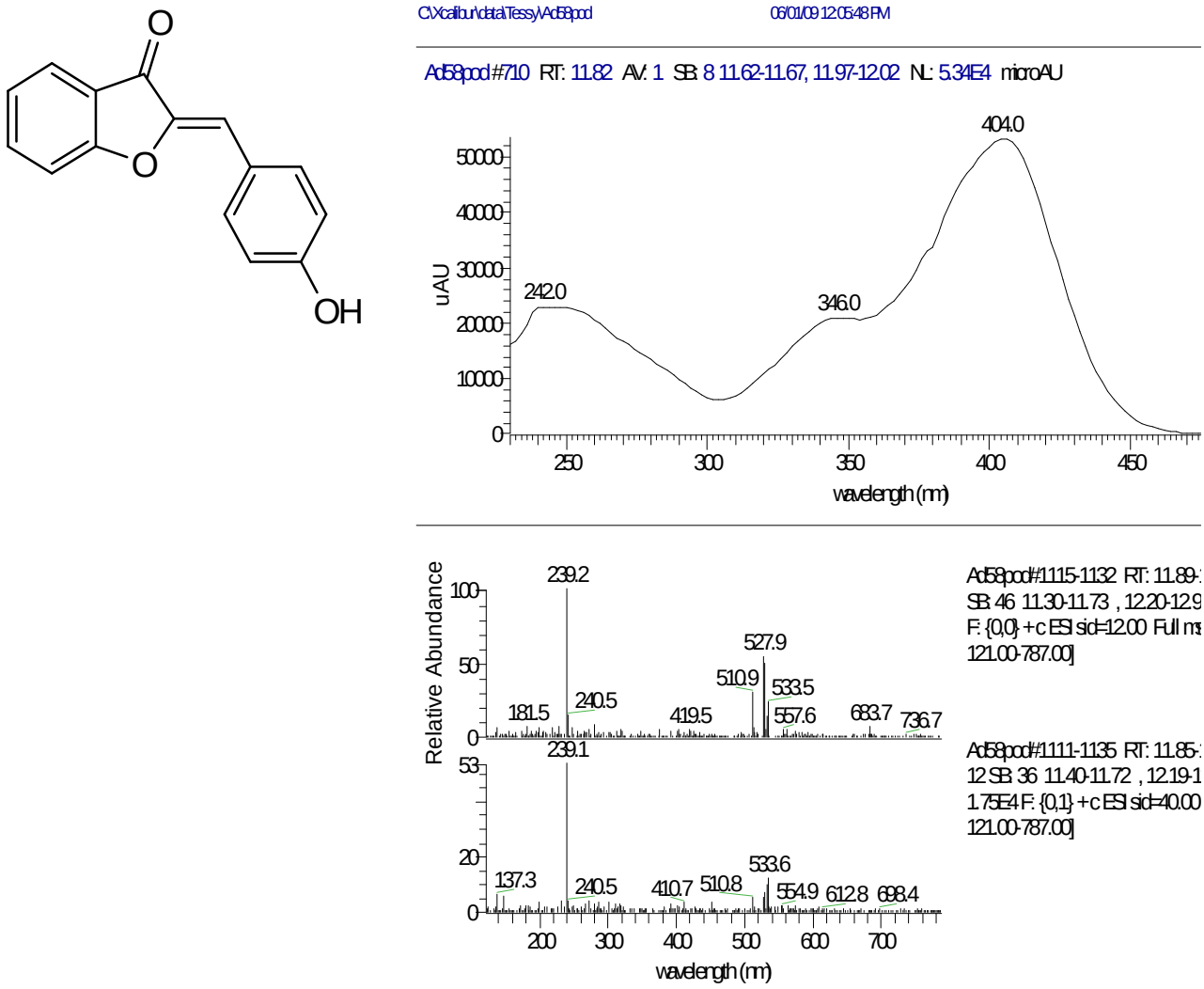

Figure 43: Structure and spectral UV-Vis and MS (M+1=239) data for 4-OH aurone

The main two products elute at around 16 min and they seem to be dimers of the starting chalcone showing the same UV-Vis properties and a MW of 478 (240X2-2+1=479) (see **Figure 44)**. Following the same arguments as in pp. 47-53 one may claim formation of a C-C bond between the sp^2 carbons of the chalcone double bond.

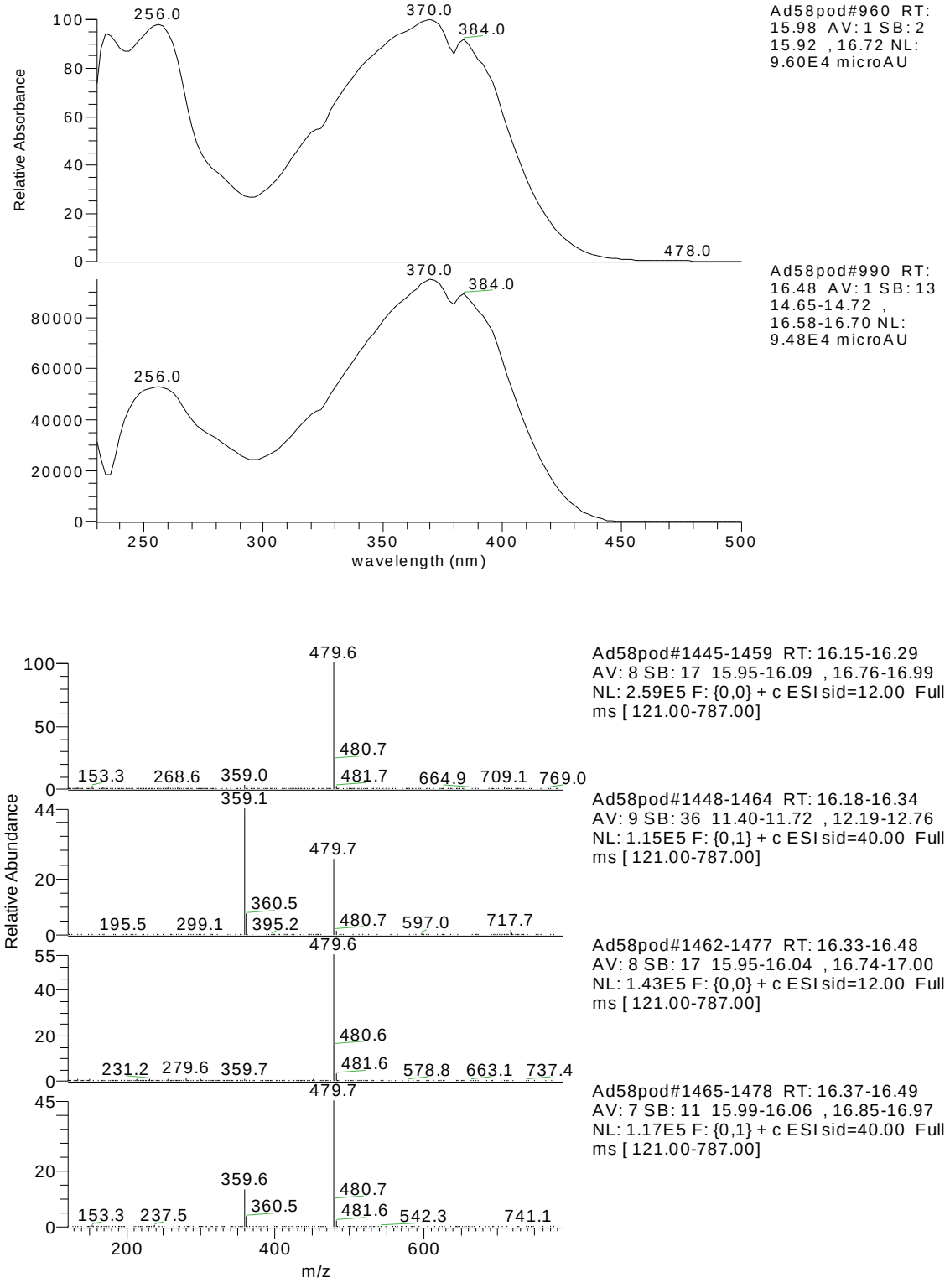

Figure 44: UV-Vis and MS spectra of the presumed chalcone dimers.

The fragment at m/z=359 is tentatively explained in **Figure 45** (for only one presumed isomeric structure) and supports the structural assumption of a chalcone dimer through a proton transfer mechanism and a Mc Lafferty-type rearrangement.

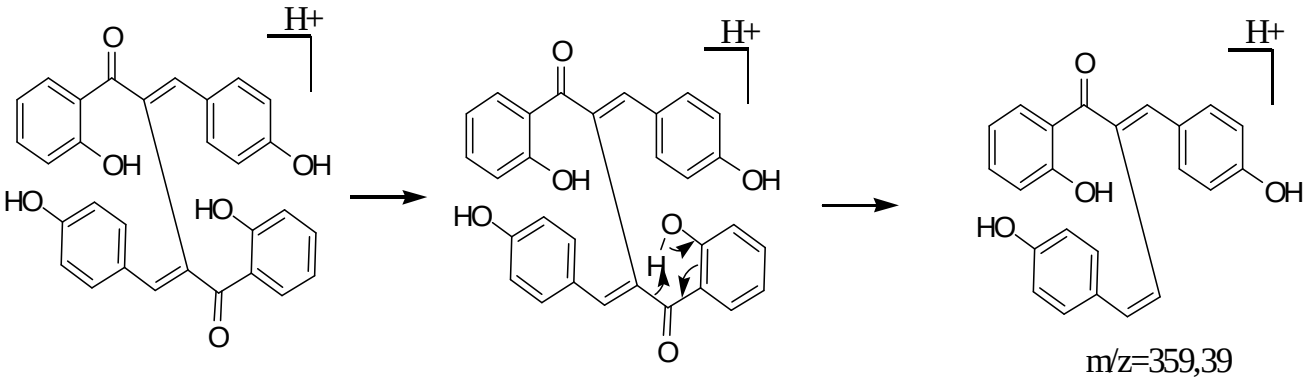

Figure 45: Mechanism for m/z=359 of the chalcone dimers.

Comparing the observations with those in pp 47 - 53 we may deduce the possibility of use of the onion POD (as crude extract and in the conditions mentioned) for olefinic sp^2 C-C bond formation, as it clearly occurred in the case of aureusidin and here in the case of the chalcone dimerisation. This finding certainly requires further investigation with many more molecules.

As we observed, the peroxidase did result in the cyclisation of the catechol-like chalcone (PHC) into the corresponding aurone, whereas the same route was not identified for the chalcone that does not bear the ortho dihydroxy system (DHC). A polyphenol oxidase would add a hydroxy group next to the existing one and then induce cyclisation (Toru et *al*, 2001). In this view and in the context of the present work, future studies must be undertaken to achieve this using various PPO sources, like from the potato.

CONCLUSION

Conclusion

In the present work the activity of crude onion peroxidase extracts was evaluated as a cheap and green tool for applications in the synthesis of fine chemicals.

First, the catalytic properties of the enzyme were monitored using protocatechuic acid as a substrate. The results obtained indicated that the enzyme showed maximum activity at 30°C, pH 6, 0.8mM H_2O_2, and 2mM substrate concentration.

Then, the conditions for optimium activity of the POD extract were further fine-tuned using Response Surface Methodology. Maximum aureusidin yield was obtained at room temperature, pH 5 and a reaction time of 5 hours. After that, scale up reactions for chalcone cyclization on PHC and DHC were carried out using the optimum parameters obtained. Indeed, aureusidin was obtained in good yield from PHC, a dimer of high regiospecificity, unknown so far to our knowledge, was also isolated and its yield found to be reaction time dependent. It is of interest to remark that the dimer does not appear in low scale experiments due, presumably, to the DMF concenrtration which is used with the enzyme. High DMF concentration seems to suppress dimer formation. DHC, which lacks the catechol system, having only one hydroxyl para to the double bond, does not cyclise into the aurone, a result expected for POD action as opposed to PPO. However, the olefinic C sp^2-sp^2 linkage seems to take place on the starting material.

The main conclusion is that indeed the crude onion POD enzyme extract may be used and further studied for the synthesis of fine chemicals, as a green and cheap alternative in the frame of organic synthetic chemistry.

BIBLIOGRAPHY

Bibliography

Abe I., Watanabe T. and Noguchi H. (2005). Chalcone synthase of type III polyketide synthase from rhubarb (*Rheum palmatum*). Proceedings of the Japan Academy 81(10), 434-440.

Ahn M. Y., Dec J., Kim J.E and Bollag J.M. (2002). Treatment of 2,4-Dichlorophenol polluted soil with free and immobilized laccase. Journal of Environmental Quality 31, 1509-1515.

Balasundram N., Ai T. Y., Sambanthamurthi R., Sundram K. and Samman S. (2005). Antioxidant properties of palm fruit extracts. Asia Pacific Journal of Clinical Nutrition 4(4), 319-324.

Benkeblia N. (2005). Free-Radical scavenging capacity and antioxidant properties of some selected onions (*Allium cepa L.*) and Garlic (*Allium sativum L.*) extracts. Brazilian Archives of Biology and Technology 48(5), 753-759.

Bradly N. (2007). The Response Surface Methodology. Indiana University Master of Science in Applied Mathematics and Computer Science Thesis.

Chan, S. W., Lee, C. Y., Yap, C. F., Wan A., W. M. and Ho, C. W. (2009). Optimization of extractions for phenolics compounds from limau purut (*Citrus hystrix*) peels. International Food Research Journal 16, 203-213.

Chen S., Vaghchhipawala Z., Li W., Asard H. and Dickman M.B. (2004). Tomato Phospholipid Hydroperoxide Glutathione Peroxidase Inhibits Cell Death Induced by Bax and Oxidative Stresses in Yeast and Plants. Plant Physiology 135, 1630–1641.

Contessotto M. G. G., Monteiro-Vitorello C. B. , Mariani P. D. S. C. and Coutinho L. L. (2001). A new member of the chalcone synthase (CHS) family in sugarcane. Genetics and Molecular Biology, 24(1-4), 257-261.

Correa R., Fenner B.P., De Campos Buzzi F., Filho V.C., and Nuneses R.J. (2008). Antinociceptive Activity and Preliminary Structure-Activity Relationship of Chalcone-Like Compounds. Z. Naturforsch 63, 830-836.

Cosio C. and Dunand C. (2009). Specific functions of individual class III peroxidase genes, Journal of Experimental Botany 60(2), 391–408.

Cuyckens F., Ma Y. L., Pocsfalvi G., Claeys M. (2000). Tandem mass spectral strategies for the structural characterization of flavonoid glycosides. Analysis 28(10), 888 – 895.

D'Archivio M., Filesi C., Di Benedetto R., Gargiulo R., Giovannini C. and Masella R. (2007). Polyphenols, dietary sources and bioavailability. Ann Istituto Superior di Sanità 43(4), 348-361.

Daayf F. and Lattanzio V (2008). Recent advances in polyphenol research. Editors: Daayf F. and Lattanzio V. Ecology and Organismal Biology, Biodiversity 1. Wiley-Blackwell Recent, Advances in Polyphenol Research, pp 37-59.

De Gara L. (2004). Class III peroxidases and ascorbate metabolism in plants. Phytochemistry Reviews 3**,** 195–205.

Delannoy E., Marmey P., Jalloul A., Etienne H., and Nicole M. (2006). Molecular Analysis of Class III Peroxidases from Cotton. Molecular Biology and Physiology. The Journal of Cotton Science 10, 53–60.

Delannoy E., Marmey P., Jalloul A., Etienne H., and Nicole M. (2005). Oxidative stress and plant cell death suppressors. Plant Biotechnology 22, 419–422.

Dickson J., Flores L., Stewart M., Leblanc R., Pati Hari N., Lee M. and Holt H. (2006). Synthesis and cytotoxic properties of chalcones: An interactive and investigative undergraduate laboratory project at the interface of chemistry and biology. Journal of Chemical Education, 83 (6), 934-936.

El Agha A., Abbeddou S. Makris D. P., Kefalas P. (2009). Biocatalytic properties of a peroxidase-active cell-free extract from onion solid wastes: caffeic acid oxidation. Biodegradation 20, 143–153.

El Agha A., Makris D. P., Kefalas P. (2008). Hydrocaffeic acid oxidation by a peroxidase homogenate from onion solid wastes. European Food Research and Technology 227, 1379–1386.

El Agha A., Makris D. P., Kefalas P. (2008). Peroxidase-Active Cell Free Extract from Onion Solid Wastes: Biocatalytic Properties and Putative Pathway of Ferulic Acid Oxidation. Journal of Bioscience and Bioengineering, 106(3), 279-285.

Ferrer, J.L, Jez, J.M, Bowman, M.E., Dixon, R.A., Noel, J.P. (1999). Structure of chalcone synthase and molecular basis of plant polyketide biosynthesis. Nature Structural Biology 6, 775-784.

Gasull E.I., Bustos M. E., and Ferretti F. H. (2005). Synthesis of 4-X- chalcones and effect of permittivity and temperature on the reaction rate. Latinoamericana de Quimica 34(1-3), 7-12.

González E. A., Nazareno M. A. and Borsarelli C. D. (2002). Enthalpy-entropy compensation effect in the chalcone formation from naringin in water-ethanol mixtures. Journal of Chemical Society, Perkin Transactions 2(12), 2052–2056.

Hijova E. (2006). Bioavailability of chalcones. Minireview: Batisl Lek Listy; 107(3), 80-84.

Hiraga S., Sasaki K., Ito H., Ohashi Y., Matsui H (2001). A Large Family of Class III Plant Peroxidases. Cell Physiology. 42(5), 462-468.

Jiménez –Contreras E., Torres-Salinas D., Moreno R. B., Banos R. R., Lopezcozar E. D. (2009). Response Surface Methodology and its application in evaluating scientific activity. Scientometrics 79(1), 201-218.

Kefalas P., Makris D.P. (2005). Exploitation of Agri-Food Solid Wastes for Recovery of High Added-Value Compounds: The case of Grape Pomace and Onion Peels. Buletinul USAMV-CN, nr. 62/2005.

Kiassos E., Mylonaki S., Makris D. P. and Kefalas P. (2009). Implementation of response surface methodology to optimize extraction of onion (*Allium cepa*) solid waste phenolics. Innovative Food Science and Emerging Technology 10, 246-252.

London J. W., Shaw L. M., Theodorsen L., and Johan H. (1982). Application of Response Surface Methodology to the Assay of Gamma-Glutamyltransferase Stromme. Clinical Chemistry. 28(5), 1140-1143.

Lopez-Molina D., Hiner A. N. P., Tudela J, Garci-Cànovas F. and Rodriguez-Lopez J. N. (2003). Enzymic removal of phenols from aqueous solution by artichoke (*Cynana scolymus L.*) Extracts. Enzyme and Microbial Technology 33, 738-742.

Mabry T.J., Markham K.R. and Thomas M.B (1970). The systematic identification of Flavonoids. Springer-Verlag.

Majdalany M. (2008). Antioxidant Activity, Insect Repellent Properties and Synthesis of Chalcones and Aurones: Cyclization of Chalcones into Aurones by Crude Onion and Potato Enzyme Extracts. Master thesis CIHEAM.

Manu B.T. and Prasada Rao U.J.S. (2002). Calcium modulated activity enhancement and thermal stability study of a cationic peroxidase purified from wheat bran. Food Chemistry 114, 66-71.

Masayoshi H., M., Eiichiro O., E., Keiko Y.S., K., Yoshikazu T., Tokuzo N. and Toru N. (2006). Biochemical characterization and mutational studies of a chalcone synthase from yellow snapdragon (*Antirrhinum majus*) flowers. Plant Biotechotechnology 23(4), 373-378.

Mylonaki S., Kiassos E., Makris D.P. (2008). Optimization of the extraction of olive (*Olea europaea*) leaf phenolics using water/ethanol- based solvent systems and response surface methodology. Analytical Bioanalytical Chemistry 392, 977-985.

Osman A., Makris D. P., Kefalas P. (2008). Investigation on biocatalytic properties of a peroxidase-active homogenate from onion solid wastes: An insight into quercetin oxidation mechanism. Process Biochemistry (43), 861-867.

Prasad Y.R., Lakshmanarao A. and Rambabu R. (2008). Synthesis and Antimicrobial Activity of Some Chalcone Derivatives. European Journal of Chemistry 5(3), 461-466.

Sakihama Y., Cohen M.F., Grace S.C. and Yamasak H. (2002). Plant phenolic antioxidant and prooxidant activities: phenolics-induced oxidative damage mediated by metals in plants. Toxicology 177 (1), 67-80.

Sato T, Nakayama T, Kikuchi S, Fukui Y, Yonekura-Sakakibara K, Ueda T, Nishino T, Tanaka Y, Kusumi T (2001). Enzymic formation of aurones in the extracts of yellow snapdragon flowers. Plant Science 160, 229-236.

Schäfer M., Dray M., Springer A., Zacharias P. and Meerholz K. (2007). Radical Cations in Electrospray Mass Spectrometry: Formation of Open-Shell Species, Examination of the Fragmentation Behaviour in ESI-MSn and Reaction Mechanism Studies by Detection of Transient Radical Cations. European Journal of Organic Chemistry 31, 5162–5174.

Sheng Cheng M., Shi Li R. and George Kenyon G. (2000). A Solid Phase Synthesis of Chalcones by Claisen-Schmidt Condensations. Chinese Chemical Letters 11(10), 851–854.

Somepalli V., Gopala K. P., Aditya L. G. and Gottumukkala V. S. (2007). Synthesis, structural revision, and biological activities of 4’-chloroaurone, a metabolite of marine brown alga Spatoglossum variable. Tetrahedron 63, 6909-6914.

Sticher L., Penel C. and Greppin H. (1981). Calcium requirement for the secretion of peroxidases by plant cell suspensions. Journal of Cell Science 48, 345-353.

Strack D. and Schliemann W. (2001). Bifunctional Polyphenol Oxidases: Novel Functions in Plant Pigment Biosynthesis. Angewandte Chemie, International Edition 40(20), 3791-3794.

Sato T, Nakayama T, Kikuchi S, Fukui Y, Yonekura-Sakakibara K, Ueda T, Nishino T, Tanaka Y, Kusumi T (2001). Enzymic formation of aurones in the extracts of yellow snapdragon flowers. Plant Science 160(2), 229-236.

Toru N. (2002). Enzymologie of Aurone Biosynthesis. Journal of Bioscience and Bioengineering 94(6), 487-491.

Toru N., Sato T., Fukui Y., Yonekura-Sakakibara K., Hayashi H., Tanaka Y., Kusumi T. and Nishino T. (2001). Specificity analysis and mechanism of aurone synthesis catalysed by aueusidin synthase, a polyphenol oxidase homolog responsable for flower coloration. FEBS Letters 499, 107-111.

Urquiaga I. and Leighton F. (2000). Plant Polyphenol Antioxidants and Oxidative Stress Biological Research 33(2), 55-64.

Valisek J., Davidek J.and Cejpek K. (2008). Biosynthesis of Food Constituents: Natural Pigments. Czech Journal of Food Science 26(2), 73-98.

Veitch N.C. (2004). Horseradish peroxidise: a modern view of a classic enzyme. Phytochemistry 65, 249-259.

Vidali M. (2001). Bioremediation. An overview. Pure Applied Chemistry 73(7), 1163-1172.

Villalobos D.A. and Buchanan I.D. (2002). Removal of aqueous phenol by *Arthomyces ramosus* peroxidase. Journal of Environmental Engineering Science 1, 65-73.

Westenburg H. E., Kon-Joo L., Sang Kook L., FONG Harry H. S., Van Breemen R. B. , Pezzuto J. M. and Kinghorn A. D. (2000). Activity-guided isolation of antioxidative constituents of *Cotinus coggygria*. Journal of natural products 63(12), 1696-1698.

Yoichi K. , Shigeyuki K. , Seigo S., Kazumi S. , Nariaki F. and Shigeru O. (2005). Metabolism of the α,β-unsaturated ketones, chalcones and trans-4-phenyl-3-buten-2-one, by rat liver

microsomes and estrogenic activity of the metabolites. Drug Metabolism and Disposition 33(8), 1115-1123.